HHS Public Access

Author manuscript

Kidney Int. Author manuscript; available in PMC 2014 October 01.

Published in final edited form as:

Kidney Int. 2014 April ; 85(4): 855–870. doi:10.1038/ki.2013.489.

Klotho has dual protective effects on cisplatin-induced acute kidney injury

Monica Chang Panesso[2], **Mingjun Shi**[1], **Han Ju Cho**[1], **Jean Paek**[1], **Jianfeng Ye**[1], **Orson W. Moe**[1,2,3], and **Ming Chang Hu**[1,2,*]

[1]Charles and Jane Pak Center for Mineral Metabolism and Clinical Research, University of Texas Southwestern Medical Center, Dallas, TX, USA

[2]Department of Internal Medicine, University of Texas Southwestern Medical Center, Dallas, TX, USA

[3]Department of Physiology, University of Texas Southwestern Medical Center, Dallas, TX, USA

Abstract

Klotho protects the kidney from ischemia-reperfusion injury, but its effect on nephrotoxins is unknown. Here we determined if Klotho protects the kidney from cisplatin toxicity. Cisplatin increased plasma creatinine and induced tubular injury, which were exaggerated in Klotho haplosufficient (*Kl*/+) and ameliorated in transgenic Klotho overexpressing (*Tg-Kl*) mice. Neutrophil gelatinase-associated lipocalin and active caspase-3 protein, and number of apoptotic cells in the kidney were higher in *Kl*/+ and lower in *Tg-Kl* compared to wild type mice. Klotho suppressed basolateral uptake of cisplatin by the normal rat kidney cell line (NRK); an effect similar to cimetidine, a known inhibitor of organic cation transport (OCT). A decrease in cell surface and total OCT2 protein and OCT activity by Klotho was mimicked by glucuronidase. The Klotho effect was attenuated by glucuronidase inhibition. On the other hand, *OCT2* mRNA was reduced by Klotho, but not β-glucuronidase. Moreover, cimetidine inhibited OCT activity but not OCT2 expression. Unlike cimetidine, Klotho reduced cisplatin-induced apoptosis from either the basolateral or apical side, and even when added after NRK cells were already loaded with cisplatin. Thus, Klotho protects the kidney against cisplatin nephrotoxicity by reduction of basolateral uptake of cisplatin by OCT2, and a direct anti-apoptotic effect independent of cisplatin uptake. Klotho may be a useful agent to prevent and treat cisplatin-induced nephrotoxicity.

Keywords

Acute Kidney Injury; Cisplatin; Glucuronidase; Kidney; Klotho; Nephrotoxicity; Organic cation transporter

*Address correspondence to: Ming Chang Hu, MD, PhD, Charles and Jane Pak Center for Mineral Metabolism and Clinical Research, and Department of Internal Medicine, The University of Texas Southwestern Medical Center, 5323 Harry Hines Blvd., Dallas, TX 75390-8885 USA, Tel: 1-214-648-9797;, ming-chang.hu@utsouthwestern.edu.

DISCLOSURE: None.

INTRODUCTION

Cisplatin (*cis*-diammine-dichloroplatinum; CDDP) is an inorganic platinum-based chemotherapeutic agent widely used for the treatment of various solid tumors.[1] However, its full clinical potential is limited by its severe adverse actions with nephrotoxicity being the most serious.[2] Based on serum creatinine (S_{Cr}), 26% of patients develop acute kidney injury (AKI) and among those with AKI, 50% patients still had elevated S_{Cr} 15 days after treatment.[3] Volume expansion and magnesium supplementation have been tried to prevent cisplatin nephrotoxicity but the results are not satisfactory.[4] Other potential approaches such as antioxidants and blockers of cisplatin transport have been tested in animal studies with sub-optimal results[5]

Klotho was initially identified as an aging suppressor,[6] and recently found to confer protection against acute ischemia reperfusion injury.[7,8] The prototypic member alpha-Klotho, simply referred to as Klotho here, is a single-pass transmembrane protein which functions as a co-receptor for fibroblast growth factor-23.[9] The extracellular domain of membrane Klotho is shed and released into the circulation.[10,11] Circulating soluble Klotho in the blood may act as an endocrine factor to exert multiple remote functions including ion channel regulation, anti-insulin action, anti-Wnt signal activity, suppression of cell senescence, and anti-oxidation.[12–14] Klotho protects the kidney against acute ischemia-reperfusion injury,[7,8] and alleviates renal fibrosis induced by acute unilateral ureteral obstruction.[15] Klotho deficiency was shown in rodents given cyclosporine,[16] cisplatin,[17] and folic acid,[17] but it is unclear whether the low Klotho is a mere biomarker reflecting injury or if it contributes to the pathogenesis of the AKI. The role of Klotho in nephrotoxic AKI needs to be elucidated.

We tested whether cisplatin induces Klotho deficiency and nephrotoxicity, examined whether Klotho overexpression attenuates cisplatin nephrotoxicity, and explored how Klotho protects kidney from cisplatin nephrotoxicity. We confirmed renal Klotho deficiency in cisplatin-injected animals. High Klotho levels effectively prevented cisplatin-induced kidney damage *in vivo* and directly protected NRK cells against cisplatin cytotoxicity *in vitro*. The renoprotection is conferred by Klotho's ability to decrease cisplatin uptake by renal tubules through inhibition of organic cation transporter (OCT), and by suppression of apoptosis induced by cisplatin.

RESULTS

Cisplatin-induced acute nephrotoxicity

When mice were given a single intraperitoneal injection of cisplatin, plasma creatinine (P_{Cr}) and BUN peaked at 2 to 10-fold of normal (Figure 1A,B) on day 7 followed by a slow decline but remained higher than that of vehicle-injected mice even by day 14, indicating incomplete recovery. Hematoxylin and eosin (H&E) stained kidney sections showed that the lesion was predominantly in cortex and outer medulla (Figure 1C) including brush border loss in proximal tubules, dilated tubules, luminal proteinaceous or cellular casts (asterisk), necrosis, and dilated renal tubules (arrow head) on day 4 (Figure 1B). These changes were more prominent on Day 7. Significant recovery ensued by day 14, but there were still a few

infiltrating inflammatory cells (black filled arrow) in the renal interstitium of cisplatin-injected *WT* mice. Index of histological damage was increased on day 4, peaked on day 7, and decreased by day 14 (Figure 1D). The alteration of renal pathological scores was parallel with changes of P_{Cr} and BUN.

Cisplatin-induced acute renal Klotho deficiency

After cisplatin injection in *WT* mice, renal Klotho protein expression was decreased on day 4, reached the lowest levels on day 7, and slowly recovered but still not to normal levels by day 14 (Figure 2A–C). Renal *Klotho* transcripts showed similar changes as that of Klotho protein but unlike Klotho protein, *Klotho* transcripts returned to normal by Day 14 (Figure 2D) suggesting that recovery of renal Klotho protein is slower.

As expected, *Kl*/+ mice had lower, and *Tg-Kl* mice, higher levels of Klotho protein in the kidney at baseline (Figure 2A–C). After cisplatin injection, renal Klotho protein was undetectable on day 4 and 7, and returned to half the level of vehicle-injected *Kl*/+ mice on day 14 (Figure 2A–C). Klotho levels in the kidneys were much lower in *Kl*/+ mice than those in *WT* mice at each time point. In contrast, renal Klotho protein levels in *Tg-Kl* mice were reduced by cisplatin, but remained higher than *WT* mice throughout study period (Figure 2A–C).

Klotho status and cisplatin nephrotoxicity

To test the pathogenic role of Klotho, we explored whether over-expression of Klotho protects kidney from cisplatin-induced nephrotoxicity. P_{Cr} and BUN levels were considerably lower in cisplatin-injected *Tg-Kl* mice; and higher in cisplatin-injected *Kl*/+ mice than that in cisplatin-injected *WT* mice (Figure 1A). Of note, P_{Cr} and BUN recovery was much slower in *Kl*/+ mice, and much faster in *Tg-Kl* mice compared to *WT* mice (Figure 1A).

There were more extensive histologic damage including brush border membrane detachment from proximal tubules, tubular casts at early phase (day 4–7) and renal tubular dilation and tubule-interstitial infiltration at later phase (day 14) in cisplatin-injected *Kl*/+ mice than cisplatin-injected *WT* mice (Figure 1B). Compared to *WT* mice, renal histological alteration was remarkably less in *Tg-Kl* mice at early phase (Figure 1B). Histological scores were lower in *Tg-Kl* mice and higher in *Kl*/+ mice compared to *WT* mice at each time point (Figure 1C). Again, cisplatin-injected *Kl*/+ mice had persistently high scores on day 14 after injection, indicating that Klotho deficiency is associated with delayed recovery.

The biomarker for AKI, neutrophil gelatinase-associated lipocalin (NGAL) was more pronouncedly increased after cisplatin injection in *Kl*/+ mice, and much less in *Tg-Kl* mice compared to *WT* mice (Figure 2A–D), suggesting that the higher Klotho protects against cisplatin nephrotoxicity.

Cisplatin-induced renal apoptosis

Cisplatin-activated apoptosis is known to play a pathogenic role in AKI[18–20] and Klotho was shown to suppress apoptosis induced by oxidative stress.[21,22] We examined apoptotic cells

with terminal dUTP nick end-labeling (TUNEL) in kidney sections. After cisplatin injection, there were appreciably more apoptotic cells in *Kl/+* mice and less in *Tg-Kl* mice compared to *WT* mice (Figure 3A,B). We next examined the expression of some key modulators of apoptosis. Because TUNEL positivity peaked on day 7, we examined the protein and mRNA levels of Bcl-2 (anti-apoptotic protein), Bax (pro-apoptotic protein), and active form of caspase-3 (a pivotal proteases in the initiation and execution of apoptosis) in the kidney.[20,23] *Tg-Kl* mice had less elevation of Bax/Bcl-2 ratio and caspase-3 protein, whereas *Kl/+* mice had higher values than *WT* mice (Figure 3C,D). Alterations of *Bax*/*Bcl-2* mRNA ratio in the kidney were similar to their protein expression levels (Figure 3E). Therefore, high renal Klotho decreases cisplatin-activated apoptosis through modulation of Bax/Bcl-2 and caspase-3 signal cascades.

Tg-Kl mice had higher population of Ki-67 positive cells (marker of cell proliferation) in the kidney at baseline, and a smaller increase after cisplatin injection compared to that in *WT* mice (Figure 3F,G), suggesting that there is higher cell proliferation with less tissue damage with the higher Klotho level. In contrast, *Kl/+* had modest but statistically fewer Ki67 positive cells in the kidney both at baseline, and after cisplatin injection compared to *WT* mice (Figure 3F,G). Reduced cell proliferation after severe tissue damage may be attributed to stem cell depletion resulting from over-activity of Wnt signal pathway in Klotho deficiency.[24]

NRK cell model of cisplatin cytotoxicity

To study the direct mechanisms of Klotho protection, we used NRK cells, a renal tubule cell line harboring both proximal and distal tubule features[25,26] *in vitro* on Transwell plates to allow separation of the apical and basolateral compartments. LDH release was higher when NRK cells were incubated with cisplatin from the basolateral compared to the apical side (Figure 4A), suggesting that cisplatin entry to NRK cells from basolateral membrane is a prerequisite for cisplatin cytotoxicity. Of note, basolateral co-incubation with either Klotho or cimetidine, a known inhibitor of the organic cation transporter-2 (OCT2), significantly reduced LDH release, but Klotho-treated cells had less LDH release compared to cimetidine-treated cells suggesting that Klotho may be more potent than cimetidine or exert actions that are beyond mere inhibition of cisplatin uptake. Furthermore, only Klotho, but not cimetidine decreased LDH release when added into apical side with cisplatin on the basolateral side (Figure 4A), again indicating that Klotho protein has protective effects beyond OCT inhibition and cisplatin uptake.

To address possible Klotho effects that are not related to modification of cisplatin uptake, NRK cells were pre-incubated with basolateral cisplatin 20 minutes when uptake is completed,[27,28] followed by wash-out of cisplatin, and then addition of either cimetidine or Klotho. LDH release was decreased only in Klotho-treated cells and not in cimetidine-treated cells. This response was similar to that seen when apical cimetidine was compared to apical Klotho (Figure 4A); further supporting that Klotho has direct cytoprotection in addition to the inhibition of cisplatin uptake.

Consistent with changes in LDH release, TUNEL staining of apoptotic cells yielded similar results. Cisplatin addition to basolateral medium triggers apoptosis (Figure 4B,C), which could be rescued by basolateral co-incubation of Klotho or cimetidine.

Klotho effect on basolateral cisplatin uptake by NRK cells

Either cimetidine or Klotho added to the basolateral compartment both protected NRK cells from cisplatin toxicity (Figure 4) suggesting that renoprotection can result at least in part from blocking cisplatin uptake. OCT2 was clearly present in total lysates from NRK cells (Figure 5A) with several bands representing the known differentially glycosylated OCT2[29,30] while OCT1 was barely detectable (Figure 5A). In contrast to protein, *OCT1* and *OCT2* transcripts were both detected in NRK cells (Figure 5B). Using Oregon Green 488-labeled fluorescent cisplatin, we found that cisplatin entered NRK cells solely from the basolateral side (Figure 5C). This uptake was blocked by addition of Klotho or cimetidine to basolateral side and not by either agent added to the apical side (Figure 5C) indicating that both Klotho and cimetidine suppressed cisplatin uptake cross the basolateral membrane. To quantify the Klotho effect on cisplatin uptake by NRK cells, we used ^{14}C-TEA as a surrogate of cisplatin to measure intracellular accumulation of ^{14}C-TEA. Cimetidine and Klotho suppressed ^{14}C-TEA uptake by NRK cells by 60.5% and 44.7% respectively on the basolateral side (Figure 5D). However the inhibitory effect was absent when ^{14}C-TEA was added to basolateral medium 20 minutes prior to either cimetidine or Klotho protein addition. When applied to the apical side, neither cimetidine nor Klotho protein, affected uptake of ^{14}C-TEA from the basolateral medium. Hence, cimetidine and Klotho effectively inhibits cisplatin entry to NRK cells from the basolateral membrane (Figure 5D).

Klotho effect on CHO cells overexpressing human OCT2

We detected low amounts of OCT2 protein in NRK and opossum kidney (OK) cells, but none whatsoever in Chinese hamster ovary (CHO) cells (Supplementary Figure 1). Therefore, we used CHO cells as hosts to transiently transfect OCT2 and/or Klotho and to study the direct effect of Klotho on OCT2 without confounding signal from endogenous OCT's. We have previously shown that Klotho inhibits the Na-coupled inorganic phosphate cotransporters NaPi-2a via its glucuronidase activity,[31] next we examined if Klotho also exerts its effect on OCT2 via similar mechanisms.

As shown in Figure 6A, suppression of ^{14}C-TEA uptake in CHO cells by Klotho could be mimicked by β-glucuronidase, but not by sialidase. The suppressive effect of Klotho and β-glucuronidase on OCT activity was blocked by the β-glucuronidase inhibitor, D-Saccharic acid 1,4-lactone (DSAL) (Figure 6A). We further studied if decrease in OCT transport activity is associated with alteration of OCT protein abundance. By immunocytochemistry, co-transfection of Klotho reduced OCT2 protein expression (Figure 6BII) compared to CHO cells transfected with OCT2 alone (Figure 6BI). Note the inverse correlation of OCT2 expression with Klotho expression (Figure 6C). β-glucuronidase alone slightly reduced OCT2 protein (Figure 6BIII) and DSAL by itself had no effect on OCT2. However, DSAL completely blocked the effect of β-glucuronidase on OCT2 protein expression (Figure 6BVI).(Figure 6BIV); and partially blunted the effect of Klotho (Figure 6BV).

Immunoblot provided more quantitative results (Figure 6D). Both Klotho and β-glucuronidase, (albeit less potently) decreased OCT2 abundance in total cell membrane pool. The reduction of OCT2 by Klotho was partially blunted but the effect of β-glucuronidase was completely blocked by DSAL (Figure 6D). Interestingly, unlike Klotho and β-glucuronidase, cimetidine only reduced ^{14}C-TEA uptake in OCT2-expressing CHO cells (Figure 6A), but did not alter OCT2 protein expression (Figure 6D), suggesting distinct mechanisms of action of cimetidine vs. Klotho and β-glucuronidase. Klotho has been shown to modify calcium channel TRPV5[32] and renal potassium channel ROMK[33] as a sialidase, so we examined whether the effect of OCT2 can also be mediated via desialidation. Addition of sialidase did not change ^{14}C-TEA uptake by OCT2 (Figure 6A) and OCT2 expression abundance in CHO cells (Figure 6D). To further examine if Klotho reduces cell surface OCT2, we specifically measured biotin-accessible OCT2. We found that Klotho reduced primarily glycosylated OCT2 on cell surface within 2 hours of addition (Supplementary Figure 2A); and reduced both glycosylated and unglycosylated OCT2 on cell surface in 2 days (Supplementary Figure 2B). Both effects were glucuronidase-dependent as they were blocked by DSAL.

To explore whether reduction of total membrane OCT2 protein in transfected CHO cells by Klotho is associated with reduction of *OCT2* mRNA, we transiently transfected human OCT2/V2 into NRK cells which have endogenous rat *oct1* and *oct2* mRNA expression and measured human *OCT2;* and rat *oct1* and *oct2* transcripts with qPCR. While native rat *oct 1* mRNA was not affect by Klotho, rat *oct2* mRNA was down-regulated by Klotho (Figure 6E). Note that the poor reactivity of anti-OCT2 antibodies does not permit us to study parallel changes in rat OCT2 protein. Interestingly, the transfected human *OCT2* transcripts which are controlled by a constitutive promoter in NRK cells were not affected at all by Klotho, suggesting that the regulation of *OCT2* mRNA levels is via transcription rather than transcript stability. Importantly, the glucuronidase inhibitor DSAL did not abolish the reduction of rat *oct2* mRNA induced by Klotho; and β-glucuronidase *per se* did not change human and rat *OCT2* mRNA. These findings indicate that Klotho affects *OCT2* transcript via a glucuronidase-independent mechanism which is distinct from its action on OCT2 protein and transport.

Klotho and renal tubular cisplatin uptake from the peritubular capillaries

To explore whether the *in vitro* Klotho effect on cisplatin uptake represents actually occurs *in vivo*, we incubated kidney slices from *Kl/+*, *WT*, and *Tg-Kl* mice with a fluorescent cationic styryl dye (ASP^+) which is a known substrate for renal OCT's.[27] ASP^+ uptake in proximal tubules was higher in *Kl/+*, and lower in *Tg-Kl* compared to *WT* mice (Figure 7). Added Klotho decreased ASP^+ uptake in the renal tubules in a manner similar to cimetidine (Figure 7). We next examined OCT1 and 2 protein and mRNA in kidneys from mice with different genetic Klotho levels.

OCT2 was exclusively expressed in basolateral side of proximal tubules (Figure 8A) in renal cortex (Supplementary Figure 3). In contrast, OCT1 was expressed in both cortex and medulla with much lower abundance compared to OCT2 (Supplementary Figure 4) and appeared to be present in apical, cytoplasmic, and basolateral compartments of both

proximal and distal tubules (Figure 8A). OCT2 may be the major candidate transporter for cisplatin uptake from basolateral side of proximal tubules.

Renal OCT1 protein expression levels was comparable among *Kl/+*, *WT*, and *Tg-Kl* mice, but the levels of OCT2 protein appeared the highest in *Kl/+* mice and lowest in *Tg-Kl* mice (Figure 8B). In *Tg-Kl* mice, OCT2 protein expression was more restricted in proximal tubules, whereas the location of OCT2 protein in renal tubules of *Kl/+* mice was similar to that of *WT* mice, except in higher abundance (Figure 8C). An analysis of *oct1* and *oct2* transcripts by RT-PCR (Figure 8D) and qPCR (Figure 8E) showed an inverse relationship between *oct2* transcript level and *Klotho* gene dose. In contrast, *oct1* appears not to be modulated by Klotho (Figure 8D).

To further explore the effect of Klotho on cisplatin transport in the kidney in intact animals, we intraperitoneally injected ^{14}C-TEA into *Kl/+*, *WT*, and *Tg-Kl* mice and measured the plasma ^{14}C-TEA clearance, urinary ^{14}C-TEA excretion and examined its distribution in several organs. *Tg-Kl* mice had higher blood ^{14}C-TEA levels (Figure 9A), and lower urinary ^{14}C-TEA excretion (Figure 9B,C) than that of *Kl/+* mice, while creatinine clearance was stable after ^{14}C-TEA injection (figure 9D). Area under the curve from 0 to 60 minutes ($AUC_{0\text{-}60\ min}$) of plasma ^{14}C-TEA were much higher in *Tg-Kl* than that in *Kl/+* mice, whereas $AUC_{0\text{-}60\ min}$ of urinary ^{14C}-TEA were much lower in *Tg-Kl* than that in *Kl/+* mice (Table 1) indicating that Klotho affects plasma ^{14}C-TEA clearance through modulation of urinary excretion. ^{14}C-TEA in the kidneys was much lower in *Tg-Kl* mice than that in *Kl/+* mice (Figure 9E), as shown by autoradiograms of frozen organ sections (Figure 9F). The high uptake in the liver may be due to hepatic OCT1 expression;[34,35] while other organs (Figure 9E,F) have less and constitutive uptake which is not regulated by Klotho. These results provided direct *in vivo* evidence that Klotho modulates cisplatin uptake by renal tubules.

DISCUSSION

Cisplatin is a powerful anti-cancer agent with nephrotoxicity being its most serious side effect.[36] Cisplatin and or its hydrated or hydroxylated metabolite are mainly excreted through the kidney.[36] Thus the kidney is exposed to high concentrations of cisplatin and its toxic metabolites which contributes to the risk of nephrotoxicity.[37] Cisplatin-induced nephrotoxicity is characterized by renal wasting of sodium, calcium, magnesium, and amino acids,[38] and by acute fall in GFR.[39] Unfortunately there is no effective means presently to prevent or/and treat this dire side effect. This study showed that cisplatin nephrotoxicity is strikingly attenuated in *Tg-Kl* mice (Figures 1 and 2). The mechanisms underlying Klotho renoprotection includes blockage of renal tubular cisplatin uptake from basolateral side by suppression of OCT2-mediated cisplatin uptake (Figures 5 to 9). In addition and independent of uptake, Klotho exerts an anti-apoptotic effect in renal tubules treated with cisplatin (Figures 3 and 4). Therefore, Klotho may be an ideal prophylactic or/and therapeutic agent to prevent and/or treat cisplatin nephrotoxicity when given before or after cisplatin.

Cisplatin-induced apoptosis has previously been documented and suppression of apoptosis was experimentally shown to protect against cisplatin cytotoxicity and nephrotoxicity.[19,20,40–43] Klotho was also known to inhibit apoptosis *in vitro*[22,44,45] and *in vivo*[7,46] This study demonstrated reduced apoptosis in kidney tissues in *Tg-Kl* mice (Figure 3A) and in kidney cell lines (Figure 4B) treated with Klotho indicating that anti-apoptosis may be one of mechanism whereby Klotho protects kidney against cisplatin nephrotoxicity. Cisplatin-induced apoptosis in kidney cells is synergistically enhanced by tumor necrosis factor (TNF)-α,[47] which causes Fas-dependent apoptosis in a variety of cell and tissue in many organs including cisplatin induced nephrotoxicity.[48,49] TNF-α working with interferon-γ suppresses Klotho expression *in vivo* and *in vitro*.[50] On the other hand, Klotho suppressed TNF-α-induced expression of intracellular adhesion molecule-1 and vascular cell adhesion molecule-1; and reversed TNF-α-induced inhibition of eNOS phosphorylation.[51] Whether the high level of membrane Klotho in *Tg-Kl* mice is associated with suppression of Fas-dependent apoptosis triggered by cisplatin remains to be defined.

The mechanism whereby cisplatin enters the cell is not completely understood. Cisplatin is hydrophilic and cellular uptake is dependent on transporter(s).[52] OCTs clearly play a key role in cisplatin influx into cells although its efflux is less well defined.[53–55] We showed strong expression of OCT2 in proximal tubules on the basolateral membrane (Figure 8) providing a portal for cisplatin entry and cytotoxicity.[56] A previous *ex vivo* study using isolated kidney perfusion showed that cisplatin transported across the basolateral side from peritubular capillary contributes to cisplatin nephrotoxicity.[57] The role of OCT2 in mediating cisplatin cytotoxicity and cisplatin nephrotoxicity was shown in cultured kidney cells from different species including human,[37,58] mouse,[58] pig,[59] opossum,[60] and dog;[61] by *ex vivo* studies with human and rat kidney slices;[62] and by *in vivo* animal studies with animals genetic deletion of OCTs,[37,63] or animals treated with OCTs inhibitors.[64]

Our *in vitro* study with normal NRK cells (Figures 4 and 5) and *ex vivo* study using kidney slices (Figure 7) showed that inhibition of cisplatin uptake from basolateral compartment by suppression of OCT2 is one mechanism whereby Klotho protects cells from cisplatin cytotoxicity. Klotho protein possesses putative enzymatic function and regulates several renal ion channels and transporters via glycan modification: Na-dependent phosphate cotransporter-IIa (NaPi-2a),[31] transient receptor potential ion channel 5 (TRPV5),[32] and renal K^+ channel renal outer medullary potassium channel 1 (ROMK1).[33] OCT2 is a glycosylated protein (Figures 5A and 8B, Supplementary Figure 1),[29] and unglycosylated OCT2 fails to transport TEA and is associated with low protein abundance in the cell surface plasma membrane suggesting glycosylation status may influence OCT2 protein expression in and targeting to the cell membrane.[30] We showed that inhibition of renal tubular cisplatin uptake by Klotho *in vitro* (Figure 5), *ex vivo* (Figure 7), and *in vivo* (Figure 9), and mechanism whereby Klotho suppresses OCT2 function is multifactorial (Figure 10). Klotho could function as glucuronidase to reduce surface and total cellular OCT2 protein, because both Klotho and β-glucuronidase decreased human OCT2/V5 protein which was blocked by DSAL (Figure 6B–D, Supplementary Figure 2). But reduction of *OCT2* mRNA is independent of glucuronidase (Figure 6E), because neither Klotho nor β-glucuronidase affected human *OCT2* mRNA (Figure 6E) supporting a regulatory mechanism at the protein

translation and/or stability level. The higher transcripts of *OCT2* in the kidneys were observed in *Kl*/+ mice and lower in *Tg-Kl* respectively, further suggesting that Klotho could also modulate OCT2 in the transcriptional level.

The mechanisms of cisplatin cytotoxicity are still not completely understood. Our data indicate that the cytoprotective effect of Klotho is not completely dependent upon cisplatin entry and suppression of apoptosis, because there was reduced cell proliferation in the kidneys of *Kl*/+ mice (Figure 3E,F), which might be due to overactivity of Wnt signal pathway and resultant stem cell depletion.[24] It is conceivable that Klotho deficiency also caused low cell proliferation with subsequent delayed tissue regeneration.

The third OCT isoform (OCT3)[65] and the copper transporter 1[66] were proposed to be involved in cisplatin transport and potentially contribute to cisplatin cytotoxicity. We did not examine the effect of Klotho on these transporters; therefore, we could not exclude any potential link of suppressive effect of Klotho on these two proteins with cytoprotective effect of Klotho.

Another issue that we did not examine is whether decreased cisplatin uptake by renal tubular cells will decrease uptake of cisplatin by tumors and impairs the anti-tumor activity of cisplatin. This is highly unlikely because: cimetidine does not have[67] or only has minimum effect[64] on the anti-tumor activity of cisplatin, and Klotho itself was recently shown to be a tumor suppressor.[15,68] Therefore, combined application of cisplatin with Klotho may decrease renal uptake and clearance and allow the same systemic levels to be achieved with a lower dose of cisplatin and potentially enhance cisplatin's anti-tumor efficacy while protecting the kidney from nephrotoxicity. One recent publication *in vitro* study revealed that overexpression of Klotho could actually sensitize cisplatin resistant lung cancer cells by induction of cell death.[69] Comparison of anti-tumor activity and nephrotoxicity of cisplatin vs. combined cisplatin and Klotho in immunodeficient mice with cancer xenograft will provide the definite answer to this important question.

Klotho is expressed in renal distal tubules, but also in renal proximal tubules albeit in lower abundance.[31] The fact that soluble Klotho could directly suppress OCT2 activity and reduce OCT2 protein (Figures 4 and 7) implies that Klotho from the distal tubule, peritubular capillary and proximal tubule can all potentially confer protection. *Tg-Kl* mice have higher blood Klotho protein than *WT* mice do.[8,70,71] The current study cannot discern whether renoprotection by Klotho is derived from circulating Klotho or from intrarenal Klotho although high soluble Klotho in blood circulation is highly likely to play renoprotective function.

In summary, this dataset supports the model that the acute Klotho deficiency induced by cisplatin is aggravating the renal injury. The mechanisms of cytoprotection of Klotho against cisplatin-induced cytotoxicity are multifaceted (summarized in Figure 10). Klotho transcriptionally and/or post-translationally decreases OCT2 protein abundance, reduces cell surface OCT2 protein, and suppresses cisplatin uptake. In addition, Klotho suppresses apoptosis induced by cisplatin and reduces cell injury. From a therapeutic point of view, Klotho's effect on blocking cisplatin uptake offers potential in utilizing Klotho as

prophylactic agent for patients. The anti-apoptotic action of Klotho may be applicable in patients who have already received cisplatin or has experienced nephrotoxicity.

METHODS

Materials and antibodies

All chemicals were obtained from Sigma-Aldrich (St. Louis, MO), except otherwise noted. Culture media, (Invitrogen, Carlsbad, CA); penicillin and streptomycin (Cambrex, East Rutherford, NJ); enhanced chemiluminescence detection kit (Amersham Biosciences, Piscataway, NJ); and nitrocellulose and polyvinylidene difluoride (PVDF) membranes (Millipore, Billerica, MA). Soluble recombinant murine Klotho protein containing the extracellular domain (amino acid number 31-982) (rMKl) with C-terminal V5 and 6xHis tags were purified from conditional medium by affinity column chromatography using anti-V5 antibody (Sigma-Aldrich, St. Louis, MO) as previous described.[8] Antibodies used were: anti-Klotho monoclonal antibody (KM2076) (gift from M. Kuro-o, Univ. Texas Southwestern Medical Center);[8] anti-OCT2 antibody from Alpha Diagnostic International (San Antonio, TX); neutrophil gelatinase-associated lipocalin (NGAL) from R&D Systems, Inc. (Minneapolis, MN); V5 and β-actin from Sigma-Aldrich, (St. Louis, MO); Bcl-2 and Bax from Santa Cruz Biotechnology (Santa Cruz, CA); Cleaved and active caspase-3 from Cell Signaling Technology (Danvers, MA); Ki-67 from Abcam Inc. (Cambridge, MA).

Experimental animals

Transgenic mice over-expressing Klotho (*Tg-Kl;* EFmKL46 line) and Klotho hypomorphic mice (*Kl/+*)[8] were maintained at the Animal Resource Center at the University of Texas Southwestern Medical Center. Mice were housed in a temperature-controlled room with a 12:12 hour light-dark cycle and were given *ad libitum* access to standard rodent chow (Teklad, 2016 from Harlan Laboratories, Inc.) and tap water throughout the study All animal work was conducted following the Guide for the Care and Use of Laboratory Animals by The National Institutes of Health and was approved by the Institutional Animal Care and Use Committee at UT Southwestern Medical Center.

Wild type (*WT*) littermates were used as controls. Background of the genetically manipulated mice is 129sv. The age of mice ranged from 12 – 14 weeks (body weight 30 – 40 g). Cisplatin (Sigma-Aldrich, St Louis, MO) (10 mg/Kg) or vehicle (sterile 0.9% NaCl) was injected intraperitoneally into male *WT*, *Kl/+* and *Tg-Kl* mice. Animals were anesthetized for euthanasia and terminal organ harvest at the indicated time points.

^{14}C-TEA kinetic study *in vivo*

Male *WT*, *Kl/+* and *Tg-Kl* mice were injected intravenously with a single dose of (10 μl/g BW) ^{14}C-tetraethylammonium (^{14}C-TEA) (0.1 mCi/ml, special activity 3.5 mCi/mmol) (Perkin-Elmer, Shelton, CT) and blood and urine samples were collected at 0, 30, 60, 90 hours post injection for determination of radioactivity with liquid scintillation counting. At 90 hours, mice were euthanized and kidney, liver, lung, spleen, muscle and heart were collected and homogenized to assay for ^{14}C-TEA uptake by scintillation counting. The

radioactivity was normalized to tissue protein. Organs were freshly frozen with liquid N_2 and sectioned for autoradiography.

ASP^+ uptake by renal tubules *ex vivo*

Kl/+, *WT* and *Tg-Kl* mice were euthanized and kidneys were collected and sliced at 6 mm and incubated with 20 μM of a cationic styryl dye (4-(4-dimethylamino)-styryl)-N-methylpyridiniu (Molecular probe, Invitrogen, Carlsbad, CA) (ASP^+, a substrate of OCT) in presence of Klotho (0.4 nM) or vehicle at 37 °C for 1 hour in high glucose-DMEM containing 10% fetal bovine serum and oxygenated with 95% O_2. Kidney slices were frozen with liquid N_2 and sectioned at 4 μm and co-stained with rhodamine-phalloidin (Molecular Probes, Eugene, OR) and rat monoclonal antibody for Klotho (KM2076). ASP^+ uptake by renal proximal tubules were visualized with fluorescent microscopy (Zeiss LSM-510 laser scanning microscope, Carl Zeiss, Advanced Imaging Microscopy, Germany).

Cell culture experiments

NRK (normal rat kidney) cells are polarized rat renal epithelial cells with mixed proximal and distal tubule features,[25,26] cultured at 37°C in a 95% air 5% CO_2 atmosphere. Cells were grown in high-glucose (450 mg/dl) DMEM supplemented with 10% fetal bovine serum, penicillin (100 U/ml), and streptomycin (100 mg/ml). NRK cells were seeded in Transwell plates (Corning Incorporated, Life Sciences, Lowell, MA) with access from apical and basolateral chambers. Leakage across the monolayer was ruled out by complete absence of ^{3}H-Inulin flux (not shown). NRK cells were rendered quiescent overnight after 100% confluence (measured transepithelial electrical resistance-0.5–1×10^5 Ω[72]) by withdrawal of serum. Cisplatin (0.1 mM) or vehicle was added to the apical or basolateral media for 4 hours. The effect of Klotho (0.4 nM) and OCT blocker cimetidine (0.1 mM) were tested. Apical and basolateral culture medium were collected for measurement of lactate dehydrogenase (LDH) release to evaluate cisplatin-induced cytotoxicity.

For measurement of OCT activity, completely confluent NRK cells in Transwell plates were exposed to ^{14}C-TEA (0.1 mCi/ml, special activity 3.5 mCi/mmol) (Perkin-Elmer, Shelton, CT) in the basolateral medium for 20 minutes with cimetidine, Klotho, or vehicle. Intracellular radioactivity was determined by scintillation counting and normalized by cell protein.

Cisplatin uptake by NRK cells

Cisplatin was conjugated to an Oregon Green 488 dye with Ulysis Nucleic Acid Labeling kit (Molecular Probes, Invitrogen, Carlsbad, CA) and purified by column chromatography based on manufacturer's instruction. NRK cells were passed in high-glucose (450 mg/dl) DMEM supplemented with 10% fetal bovine serum, penicillin (100 U/ml), and streptomycin (100 mg/ml). Cells were incubated with fluorescent cisplatin using Transwell plates and signal was detected by fluorescent microscopy (Zeiss LSM-510 laser scanning microscope, Carl Zeiss, Advanced Imaging Microscopy, Germany).

Transient transfection in Chinese hamster ovary (CHO) cells

Full length open reading frame of human membrane Klotho (Gene bank access number: NM 004795) was subcloned to pcDNA3.1(+) expression vector (Invitrogen, Carlsbad, CA). One deca-histidine tag was inserted into N-terminus of human Klotho (10His-Klotho) and confirmed by sequencing analysis. The V5 tagged-human OCT2 (OCT2/V5) plasmid was kindly provided by Dr. Stephen Wright (University of Arizona, Tuczon AR).[73] Transiently transfections were performed with Lipofectamine 2000 (Invitrogen, Carlsbad, CA) into CHO cells (ATCC, Manassas, VA) which do not express endogenous OCT2 or Klotho. CHO cells were grown in 50:50 Ham's F12/high-glucose (450 mg/dl):DMEM (Molecular probe, Invitrogen, Carlsbad, CA) supplemented with 10% fetal bovine serum, penicillin (100 U/ml), and streptomycin (100 mg/ml) (Molecular probe, Invitrogen, Carlsbad, CA) and maintained in a humidified atmosphere with 5% CO_2. After 48 hours post-transfection, cells were subjected to RT-PCR, immunoblot, immunocytochemistry and ^{14}C-TEA uptake experiments.

Total cell membrane preparation from CHO cells

Total cell membrane protein was extracted based on published methods.[30,74] Two days after transient transfection, CHO cells were scraped and homogenized in alkaline solution [pH 11.5, 100 mM $NaCO_3$] containing phosphatase inhibitors and protease inhibitor cocktails (Roche Diagnostics, Indianapolis, IN) by passing 27-gauge needle. After low speed centrifugation (400×g, 10 min), debris was discarded, and supernatant were centrifuged (109,000×*g*, 30 min, 2°C, Beckman TLX/TLA 100.3 rotor, Fullerton, CA) and pellets were resuspended in RIPA containing protease inhibitor cocktails and phosphatase inhibitors. Protein concentration was determined by the Bradford method (Bio-Rad Laboratories, Hercules, CA). Fifty μg protein of total membrane proteins was electrophoretically fractioned, transferred and immunoblotted by V5, KM2076, or β-actin antibody sequentially.

Kidney histology, histopathology, and immunohistochemistry

Four μm sections of paraffin embedded kidneys were subjected to Hematoxylin and Eosin (H&E) staining for kidney histology. The H&E stained kidney sections were photographed by one of the investigators blinded to the experimental protocol using an Axioplan 2 Imaging system (Carl Zeiss Micro-Imaging, Inc. Thornwood, NY). A semi-quantitative pathological scoring system was used as described with minor modification[8]. The severity of renal damage was scored with a grading system (0, 1, 2, 3). 0 = no visible lesions, normal or near normal kidney morphology; 1 = mild dilation in some tubules, cell swelling, luminal debris (cast), and nuclear condensation, partial loss of brush border membranes in <1/3 tubules in high field; 2 = obvious dilation of many tubules, loss of brush border membranes, nuclear loss, and cast in <2/3 tubules in high field; 3: severe dilation of most tubules, total loss of brush border membranes, and nuclear loss in >2/3 tubules in high field. Ten fields (40x) were counted for cortex and outer stripe of outer medulla in each kidney section. Thus, the total score for each kidney was calculated by addition of all scores from 100 fields with a maximum score of 300.

For immunohistochemistry, kidney sections (4μm) were permeabilized in Triton X-100 (0.1% in PBS, 3 min), and antigens were retrieved, and blocked. Specimens were incubated

with primary antibodies overnight at 4°C, followed by incubation with different fluorophore-conjugated secondary antibodies (Invitrogen, Carlsbad, CA) for 60 minutes. Sections were visualized with a Zeiss LSM-510 laser scanning microscope (Carl Zeiss, Advanced Imaging Microscopy, Germany). TUNEL assay was used to detect apoptotic cells with *in situ* cell death detection kit (Roche Diagnostics, Indianapolis, IN), nuclei were stained with DAPI and visualized with a Zeiss LSM-510 laser scanning microscope (Carl Zeiss, Advanced Imaging Microscopy, Germany).

Plasma creatinine and BUN measurement

After euthanization, venopuncture was performed with heparinized glass capillary tubes. Plasma creatinine was measured by capillary electrophoresis.[75] Briefly, protein in the plasma was depleted with 5% trichloracetic acid precipitation, and supernatant was extracted for creatinine assay with P/ACE MDQ capillary electrophoresis system (Beckman Coulter, Inc., Fullerton, CA). Creatinine is detected at 214 nm. Plasma BUN measurement was run on Vitros 250 Chemistry System (Ortho-Clinical Diagnostics, Raritan, NJ) in The Mouse Metabolic Phenotyping Core at UT Southwestern Medical Center.

RNA extraction, RT-PCR and real time qPCR

Total RNA was extracted with RNAeasy kit (Qiagen, Germantown, MD) from NRK cells or rodent kidney tissues as described.[31] Complementary DNA (cDNA) was generated with oligo-dT primers (SuperScript III First Strand Synthesis System, Invitrogen, Carlsbad, CA) according to manufacturer's protocol. Primers used for detection of β-actin, Klotho, and cyclophilin were described in previous publications.[8] PCR products were analyzed by 2% agarose ethidium bromide gel electrophoresis. Other primers used for qPCR to detect Bcl-2, Bax, and caspase-3 were 5′-GAG ACA GCC AGG AGA AAT CA-3′ and 5′-CCT GTG GAT GAC TGA GTA CC-3′; 5′-GCT AGC AAA CTG GTG CTC AA-3′ and 5′-GAG GAC TCC AGC CAC AAA GA-3′; and 5′-GGA TAG TGT TTC TAA GGA AGA-3′ and 5′-GGC AGT AGT CGC CTC TGA AG-3′ respectively. Primers for detection of rodent OCT1 and OCT2 were 5′-GTA TGA GGT GGA CTG GAA CC-3′ and 5′-GCC CAA GTT CAC ACA GGA CT-3′; and 5′-CAG AGG AGC TGA ACT ACA CCG T-3′ and 5′-ACA GTG GGT CCA CAC AGT CA-3′; those of human OCT2 5′-GAA TTT GTT GGG CGG AGA TA-3′ and 5′-CAC CAG GAG CCC AAC TGT AT-3′ respectively with conditions described in the literature.[8] Briefly, PCR was performed in an ABI Prism 7000 Sequence Detector (Applied BioSystems, Foster City, CA), with one cycle (95°C for 10 min) and then 40 cycles (95°C for 15 s and 60°C for 1 min) in triplicate for each sample. PCR products were verified by gel electrophoresis. The cycle threshold (Ct) values of the samples were calculated and target gene transcript levels analyzed and normalized to Ct of cyclophilin. The relative abundance of target gene transcript was represented by the $2^{-\Delta\Delta ct}$ vs. control group.

LDH and TUNEL assays in NRK cells

At designated time points, culture medium was collected and immediately centrifuged at 4°C (1400 g × 5 min) to remove cells and cellular debris. Supernatants were harvested for measurement of LDH release with LDH cytotoxicity detection kit (Clontech Laboratories

Inc., Mountain View, CA) according to manufacturer's instructions. For TUNEL staining, NRK cells were seeded on glass cover slips in 12-well plates and treated as mentioned above. After removal of culture medium, cells were rinsed with pre-chilled PBS thrice and fixed in 4% paraformaldehyde (PFA) for 20 minutes. Apoptotic cells were detected with *in situ* cell death detection kit (Roche Diagnostics, Indianapolis, IN) according to manufacturer's instructions. NRK cells were co-stained with DAPI and visualized with a Zeiss LSM-510 laser scanning microscope (Carl Zeiss, Advanced Imaging Microscopy, Germany).

Immunoblot

Protein from kidney lysates and cell lysates were immunoblotted as described previously. Briefly, human or rodent kidney tissues, or NRK cells were homogenized in RIPA buffer [150 mM NaCl, 50 mM Tris·HCl, pH 7.4, 5 mM EDTA, 1% Triton X-100, 0.5% deoxycholate, and 0.1% SDS] containing fresh protease inhibitors and cleared by centrifugation (14,000×g, 4°C, 30 min). Sixty μg of protein were fractionated by SDS-PAGE, and electrophoretically transferred to polyvinylidene difluoride (PVDF) membranes. After blocking in nonfat milk, membranes were probed with primary antibodies (KM 2076 and anti-NGAL, Bcl-2 and Bax) overnight at 4°C followed by secondary antibodies conjugated with horseradish peroxidase and signal was visualized by enhanced chemiluminescence (Amersham Life Sciences). Protein abundance was quantified by densitometry using the Scion/NIH Image J software (Scion, Frederick, MD).

Statistical analyses

Data are expressed as means ± SD. Statistical analysis was performed using unpaired *Student's t*-test, or analysis of variance (ANOVA) followed by Student-Newman-Keuls test whenever appropriate. A p value of ≤0.05 was considered statistically significant. Unless otherwise stated, representative figures reflect the results in a minimum of three independent experiments.

Supplementary Material

Refer to Web version on PubMed Central for supplementary material.

Acknowledgments

Parts of these results were published in abstract form in the *Journal of the American Society of Nephrology (22: 116A, 2011)*. This work was in part supported by the National Institutes of Health (R01-DK092461 and R01-091392; R01-DK091393), O'Brien Kidney Research Center (NIH P30DK-07938), the Simmons Family Foundation, and the Charles and Jane Pak Foundation. The authors are grateful to Dr. Dihua Zhang for assistance in evaluation of kidney histology, Dr. Stephen Wright for kindly providing human OCT2-V5 plasmid, Ms Jessica Lucas for plasma creatinine determination, and Ms Kierste Miller for technical assistance.

References

1. Lippman AJ, Helson C, Helson L, et al. Clinical trials of cis-diamminedichloroplatinum (NSC-119875). Cancer Chemother Rep. 1973; 57:191–200. [PubMed: 4126381]
2. Hardaker WT Jr, Stone RA, McCoy R. Platinum nephrotoxicity. Cancer. 1974; 34:1030–1032. [PubMed: 4421400]

3. Gaspari F, Cravedi P, Mandala M, et al. Predicting cisplatin-induced acute kidney injury by urinary neutrophil gelatinase-associated lipocalin excretion: a pilot prospective case-control study. Nephron Clin Pract. 2010; 115:c154–160. [PubMed: 20407275]
4. Launay-Vacher V, Rey JB, Isnard-Bagnis C, et al. Prevention of cisplatin nephrotoxicity: state of the art and recommendations from the European Society of Clinical Pharmacy Special Interest Group on Cancer Care. Cancer Chemother Pharmacol. 2008; 61:903–909. [PubMed: 18317762]
5. Yao X, Panichpisal K, Kurtzman N, et al. Cisplatin nephrotoxicity: a review. Am J Med Sci. 2007; 334:115–124. [PubMed: 17700201]
6. Kuro-o M, Matsumura Y, Aizawa H, et al. Mutation of the mouse klotho gene leads to a syndrome resembling ageing. Nature. 1997; 390:45–51. [PubMed: 9363890]
7. Sugiura H, Yoshida T, Tsuchiya K, et al. Klotho reduces apoptosis in experimental ischaemic acute renal failure. Nephrol Dial Transplant. 2005; 20:2636–2645. [PubMed: 16204278]
8. Hu MC, Shi M, Zhang J, et al. Klotho deficiency is an early biomarker of renal ischemia-reperfusion injury and its replacement is protective. Kidney Int. 2010; 78:1240–1251. [PubMed: 20861825]
9. Matsumura Y, Aizawa H, Shiraki-Iida T, et al. Identification of the human klotho gene and its two transcripts encoding membrane and secreted klotho protein. Biochem Biophys Res Commun. 1998; 242:626–630. [PubMed: 9464267]
10. Chen CD, Podvin S, Gillespie E, et al. Insulin stimulates the cleavage and release of the extracellular domain of Klotho by ADAM10 and ADAM17. Proc Natl Acad Sci U S A. 2007; 104:19796–19801. [PubMed: 18056631]
11. Bloch L, Sineshchekova O, Reichenbach D, et al. Klotho is a substrate for alpha-, beta- and gamma-secretase. FEBS Lett. 2009; 583:3221–3224. [PubMed: 19737556]
12. Hu MC, Moe OW. Klotho as a potential biomarker and therapy for acute kidney injury. Nature reviews Nephrology. 2012; 8:423–429.
13. Hu MC, Shi M, Cho HJ, et al. The erythropoietin receptor is a downstream effector of Klotho-induced cytoprotection. Kidney Int. 2013 May 1. Epub ahead of print. 10.1038/ki.2013.1149
14. Hu MC, Shiizaki K, Kuro-o M, et al. Fibroblast growth factor 23 and Klotho: physiology and pathophysiology of an endocrine network of mineral metabolism. Annu Rev Physiol. 2013; 75:503–533. [PubMed: 23398153]
15. Doi S, Zou Y, Togao O, et al. Klotho inhibits transforming growth factor-beta1 (TGF-beta1) signaling and suppresses renal fibrosis and cancer metastasis in mice. J Biol Chem. 2011; 286:8655–8665. [PubMed: 21209102]
16. Yoon HE, Ghee JY, Piao S, et al. Angiotensin II blockade upregulates the expression of Klotho, the anti-ageing gene, in an experimental model of chronic cyclosporine nephropathy. Nephrol Dial Transplant. 2011; 26:800–813. [PubMed: 20813770]
17. Moreno JA, Izquierdo MC, Sanchez-Nino MD, et al. The inflammatory cytokines TWEAK and TNFalpha reduce renal klotho expression through NFkappaB. J Am Soc Nephrol. 2011; 22:1315–1325. [PubMed: 21719790]
18. Havasi A, Borkan SC. Apoptosis and acute kidney injury. Kidney Int. 2011; 80:29–40. [PubMed: 21562469]
19. Salahudeen AK, Haider N, Jenkins J, et al. Antiapoptotic properties of erythropoiesis-stimulating proteins in models of cisplatin-induced acute kidney injury. Am J Physiol Renal Physiol. 2008; 294:F1354–1365. [PubMed: 18385271]
20. Wei Q, Dong G, Franklin J, et al. The pathological role of Bax in cisplatin nephrotoxicity. Kidney Int. 2007; 72:53–62. [PubMed: 17410096]
21. Sugiura H, Yoshida T, Mitobe M, et al. Klotho reduces apoptosis in experimental ischaemic acute kidney injury via HSP-70. Nephrol Dial Transplant. 2010; 25:60–68. [PubMed: 19745103]
22. Ikushima M, Rakugi H, Ishikawa K, et al. Anti-apoptotic and anti-senescence effects of Klotho on vascular endothelial cells. Biochem Biophys Res Commun. 2006; 339:827–832. [PubMed: 16325773]
23. Wang J, Pabla N, Wang CY, et al. Caspase-mediated cleavage of ATM during cisplatin-induced tubular cell apoptosis: inactivation of its kinase activity toward p53. Am J Physiol Renal Physiol. 2006; 291:F1300–1307. [PubMed: 16849690]

24. Liu H, Fergusson MM, Castilho RM, et al. Augmented Wnt signaling in a mammalian model of accelerated aging. Science. 2007; 317:803–806. [PubMed: 17690294]
25. Fukuishi N, Gemba M. Use of cultured renal epithelial cells for the study of cisplatin toxicity. Jpn J Pharmacol. 1989; 50:247–249. [PubMed: 2570174]
26. Sugiura H, Yoshida T, Shiohira S, et al. Reduced Klotho Expression Level in Kidney Aggravates Renal Interstitial Fibrosis. Am J Physiol Renal Physiol. 2012
27. Horbelt M, Wotzlaw C, Sutton TA, et al. Organic cation transport in the rat kidney in vivo visualized by time-resolved two-photon microscopy. Kidney Int. 2007; 72:422–429. [PubMed: 17495857]
28. Liang XJ, Shen DW, Chen KG, et al. Trafficking and localization of platinum complexes in cisplatin-resistant cell lines monitored by fluorescence-labeled platinum. J Cell Physiol. 2005; 202:635–641. [PubMed: 15546142]
29. Burckhardt G, Wolff NA. Structure of renal organic anion and cation transporters. Am J Physiol Renal Physiol. 2000; 278:F853–866. [PubMed: 10836973]
30. Pelis RM, Suhre WM, Wright SH. Functional influence of N-glycosylation in OCT2-mediated tetraethylammonium transport. Am J Physiol Renal Physiol. 2006; 290:F1118–1126. [PubMed: 16368738]
31. Hu MC, Shi M, Zhang J, et al. Klotho: a novel phosphaturic substance acting as an autocrine enzyme in the renal proximal tubule. FASEB J. 2010; 24:3438–3450. [PubMed: 20466874]
32. Chang Q, Hoefs S, van der Kemp AW, et al. The beta-glucuronidase klotho hydrolyzes and activates the TRPV5 channel. Science. 2005; 310:490–493. [PubMed: 16239475]
33. Cha SK, Hu MC, Kurosu H, et al. Regulation of renal outer medullary potassium channel and renal K(+) excretion by Klotho. Mol Pharmacol. 2009; 76:38–46. [PubMed: 19349416]
34. Wang DS, Jonker JW, Kato Y, et al. Involvement of organic cation transporter 1 in hepatic and intestinal distribution of metformin. J Pharmacol Exp Ther. 2002; 302:510–515. [PubMed: 12130709]
35. Green RM, Lo K, Sterritt C, et al. Cloning and functional expression of a mouse liver organic cation transporter. Hepatology. 1999; 29:1556–1562. [PubMed: 10216142]
36. Goldstein RS, Mayor GH. Minireview. The nephrotoxicity of cisplatin. Life Sci. 1983; 32:685–690. [PubMed: 6338333]
37. Jonker JW, Wagenaar E, Van Eijl S, et al. Deficiency in the organic cation transporters 1 and 2 (Oct1/Oct2 [Slc22a1/Slc22a2]) in mice abolishes renal secretion of organic cations. Mol Cell Biol. 2003; 23:7902–7908. [PubMed: 14560032]
38. Blachley JD, Hill JB. Renal and electrolyte disturbances associated with cisplatin. Ann Intern Med. 1981; 95:628–632. [PubMed: 7027859]
39. Chopra S, Kaufman JS, Jones TW, et al. Cis-diamminedichlorplatinum-induced acute renal failure in the rat. Kidney Int. 1982; 21:54–64. [PubMed: 7200546]
40. Wei Q, Dong G, Yang T, et al. Activation and involvement of p53 in cisplatin-induced nephrotoxicity. Am J Physiol Renal Physiol. 2007; 293:F1282–1291. [PubMed: 17670903]
41. Molitoris BA, Dagher PC, Sandoval RM, et al. siRNA targeted to p53 attenuates ischemic and cisplatin-induced acute kidney injury. J Am Soc Nephrol. 2009; 20:1754–1764. [PubMed: 19470675]
42. Jiang M, Wang CY, Huang S, et al. Cisplatin-induced apoptosis in p53-deficient renal cells via the intrinsic mitochondrial pathway. Am J Physiol Renal Physiol. 2009; 296:F983–993. [PubMed: 19279129]
43. Han X, Yue J, Chesney RW. Functional TauT protects against acute kidney injury. J Am Soc Nephrol. 2009; 20:1323–1332. [PubMed: 19423693]
44. Medici D, Razzaque MS, Deluca S, et al. FGF-23-Klotho signaling stimulates proliferation and prevents vitamin D-induced apoptosis. J Cell Biol. 2008; 182:459–465. [PubMed: 18678710]
45. Mitobe M, Yoshida T, Sugiura H, et al. Oxidative stress decreases klotho expression in a mouse kidney cell line. Nephron Exp Nephrol. 2005; 101:e67–74. [PubMed: 15976510]

46. Haruna Y, Kashihara N, Satoh M, et al. Amelioration of progressive renal injury by genetic manipulation of Klotho gene. Proc Natl Acad Sci U S A. 2007; 104:2331–2336. [PubMed: 17287345]
47. Benedetti G, Fredriksson L, Herpers B, et al. TNF-alpha-mediated NF-kappaB survival signaling impairment by cisplatin enhances JNK activation allowing synergistic apoptosis of renal proximal tubular cells. Biochem Pharmacol. 2013; 85:274–286. [PubMed: 23103562]
48. Linkermann A, Himmerkus N, Rolver L, et al. Renal tubular Fas ligand mediates fratricide in cisplatin-induced acute kidney failure. Kidney Int. 2011; 79:169–178. [PubMed: 20811331]
49. Tsuruya K, Ninomiya T, Tokumoto M, et al. Direct involvement of the receptor-mediated apoptotic pathways in cisplatin-induced renal tubular cell death. Kidney Int. 2003; 63:72–82. [PubMed: 12472770]
50. Thurston RD, Larmonier CB, Majewski PM, et al. Tumor necrosis factor and interferon-gamma down-regulate Klotho in mice with colitis. Gastroenterology. 2010; 138:1384–1394. 1394 e1381–1382. [PubMed: 20004202]
51. Maekawa Y, Ishikawa K, Yasuda O, et al. Klotho suppresses TNF-alpha-induced expression of adhesion molecules in the endothelium and attenuates NF-kappaB activation. Endocrine. 2009; 35:341–346. [PubMed: 19367378]
52. Gately DP, Howell SB. Cellular accumulation of the anticancer agent cisplatin: a review. Br J Cancer. 1993; 67:1171–1176. [PubMed: 8512802]
53. Zhang L, Dresser MJ, Chun JK, et al. Cloning and functional characterization of a rat renal organic cation transporter isoform (rOCT1A). J Biol Chem. 1997; 272:16548–16554. [PubMed: 9195965]
54. Schomig E, Spitzenberger F, Engelhardt M, et al. Molecular cloning and characterization of two novel transport proteins from rat kidney. FEBS Lett. 1998; 425:79–86. [PubMed: 9541011]
55. Mooslehner KA, Allen ND. Cloning of the mouse organic cation transporter 2 gene, Slc22a2, from an enhancer-trap transgene integration locus. Mamm Genome. 1999; 10:218–224. [PubMed: 10051314]
56. Safirstein R, Winston J, Goldstein M, et al. Cisplatin nephrotoxicity. Am J Kidney Dis. 1986; 8:356–367. [PubMed: 3538859]
57. Miura K, Goldstein RS, Pasino DA, et al. Cisplatin nephrotoxicity: role of filtration and tubular transport of cisplatin in isolated perfused kidneys. Toxicology. 1987; 44:147–158. [PubMed: 3564050]
58. Cilenti L, Kyriazis GA, Soundarapandian MM, et al. Omi/HtrA2 protease mediates cisplatin-induced cell death in renal cells. Am J Physiol Renal Physiol. 2005; 288:F371–379. [PubMed: 15454391]
59. Okuda M, Tsuda K, Masaki K, et al. Cisplatin-induced toxicity in LLC-PK1 kidney epithelial cells: role of basolateral membrane transport. Toxicol Lett. 1999; 106:229–235. [PubMed: 10403667]
60. Endo T, Kimura O, Sakata M. Carrier-mediated uptake of cisplatin by the OK renal epithelial cell line. Toxicology. 2000; 146:187–195. [PubMed: 10814851]
61. Ludwig T, Riethmuller C, Gekle M, et al. Nephrotoxicity of platinum complexes is related to basolateral organic cation transport. Kidney Int. 2004; 66:196–202. [PubMed: 15200426]
62. Vickers AE, Rose K, Fisher R, et al. Kidney slices of human and rat to characterize cisplatin-induced injury on cellular pathways and morphology. Toxicol Pathol. 2004; 32:577–590. [PubMed: 15603542]
63. Filipski KK, Mathijssen RH, Mikkelsen TS, et al. Contribution of organic cation transporter 2 (OCT2) to cisplatin-induced nephrotoxicity. Clin Pharmacol Ther. 2009; 86:396–402. [PubMed: 19625999]
64. Franke RM, Kosloske AM, Lancaster CS, et al. Influence of Oct1/Oct2-deficiency on cisplatin-induced changes in urinary N-acetyl-beta-D-glucosaminidase. Clin Cancer Res. 2010; 16:4198–4206. [PubMed: 20601443]
65. Li Q, Peng X, Yang H, et al. Contribution of organic cation transporter 3 to cisplatin cytotoxicity in human cervical cancer cells. J Pharm Sci. 2012; 101:394–404. [PubMed: 21905038]
66. Pabla N, Murphy RF, Liu K, et al. The copper transporter Ctr1 contributes to cisplatin uptake by renal tubular cells during cisplatin nephrotoxicity. Am J Physiol Renal Physiol. 2009; 296:F505–511. [PubMed: 19144690]

67. Katsuda H, Yamashita M, Katsura H, et al. Protecting Cisplatin-induced nephrotoxicity with cimetidine does not affect antitumor activity. Biol Pharm Bull. 2010; 33:1867–1871. [PubMed: 21048313]

68. Abramovitz L, Rubinek T, Ligumsky H, et al. KL1 internal repeat mediates klotho tumor suppressor activities and inhibits bFGF and IGF-I signaling in pancreatic cancer. Clin Cancer Res. 2011; 17:4254–4266. [PubMed: 21571866]

69. Wang Y, Chen L, Huang G, et al. Klotho sensitizes human lung cancer cell line to cisplatin via PI3k/Akt pathway. PLoS One. 2013; 8:e57391. [PubMed: 23437382]

70. Kurosu H, Yamamoto M, Clark JD, et al. Suppression of aging in mice by the hormone Klotho. Science. 2005; 309:1829–1833. [PubMed: 16123266]

71. Hu MC, Shi M, Zhang J, et al. Klotho deficiency causes vascular calcification in chronic kidney disease. J Am Soc Nephrol. 2011; 22:124–136. [PubMed: 21115613]

72. Kelly KJ, Wu P, Patterson CE, et al. LOX-1 and inflammation: a new mechanism for renal injury in obesity and diabetes. Am J Physiol Renal Physiol. 2008; 294:F1136–1145. [PubMed: 18322020]

73. Barendt WM, Wright SH. The human organic cation transporter (hOCT2) recognizes the degree of substrate ionization. J Biol Chem. 2002; 277:22491–22496. [PubMed: 11953440]

74. Pelis RM, Hartman RC, Wright SH, et al. Influence of estrogen and xenoestrogens on basolateral uptake of tetraethylammonium by opossum kidney cells in culture. J Pharmacol Exp Ther. 2007; 323:555–561. [PubMed: 17684116]

75. Zinellu A, Caria MA, Tavera C, et al. Plasma creatinine and creatine quantification by capillary electrophoresis diode array detector. Anal Biochem. 2005; 342:186–193. [PubMed: 15927140]

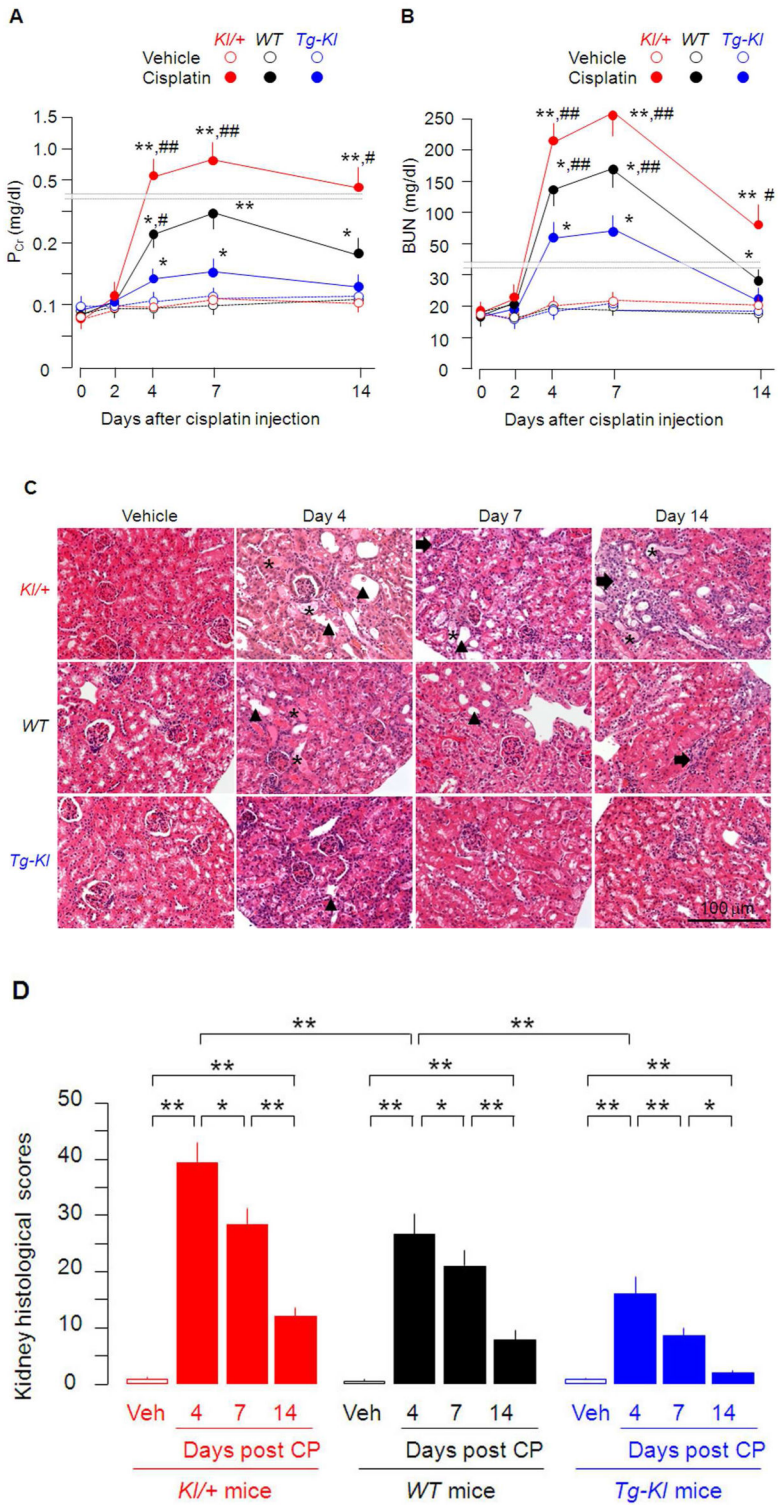

Figure 1. Cisplatin induces acute kidney injury

Cisplatin nephrotoxicity was induced by intraperitoneal injection of cisplatin (10 mg/kg body weight) or vehicle (same volume of 0.9% NaCl) once into mice with three different Klotho genetic backgrounds. (**A**) Plasma creatinine (P_{Cr}) and (**B**) BUN were measured at

days 0, 2, 4, 7, and 14 post injection. The results are expressed as means ± SD of 8 animals from each group. Statistical significance was assessed by one-way ANOVA followed by Student-Newman-Keuls test, and significant differences were accepted when *P<0.05; **:P<0.01 vs *WT* cisplatin injection; $^{\#}$P<0.05; $^{\#\#}$P<0.01 vs *Tg-Kl* cisplatin injection. At Day 4, 7, and 14 post cisplatin or vehicle injections, mice were euthanized and the kidneys were harvested and sectioned for histology from 4 animals in each group (**C**) Representative H&E staining in paraffin-embedded kidney sections. Renal tubular casts (asterisk); dilated renal tubules (arrow head); and infiltrated inflammatory (arrow). (**D**) Kidney histological scores were obtained from kidneys H&E staining by a nephropathologist blinded to the experimental conditions. Results of pathologic scores are expressed as means ± SD of 8 animals from each group. Statistical significance was assessed by one-way ANOVA followed by Student-Newman-Keuls test, and significant differences were accepted when *P<0.05; **P<0.01 between two groups.

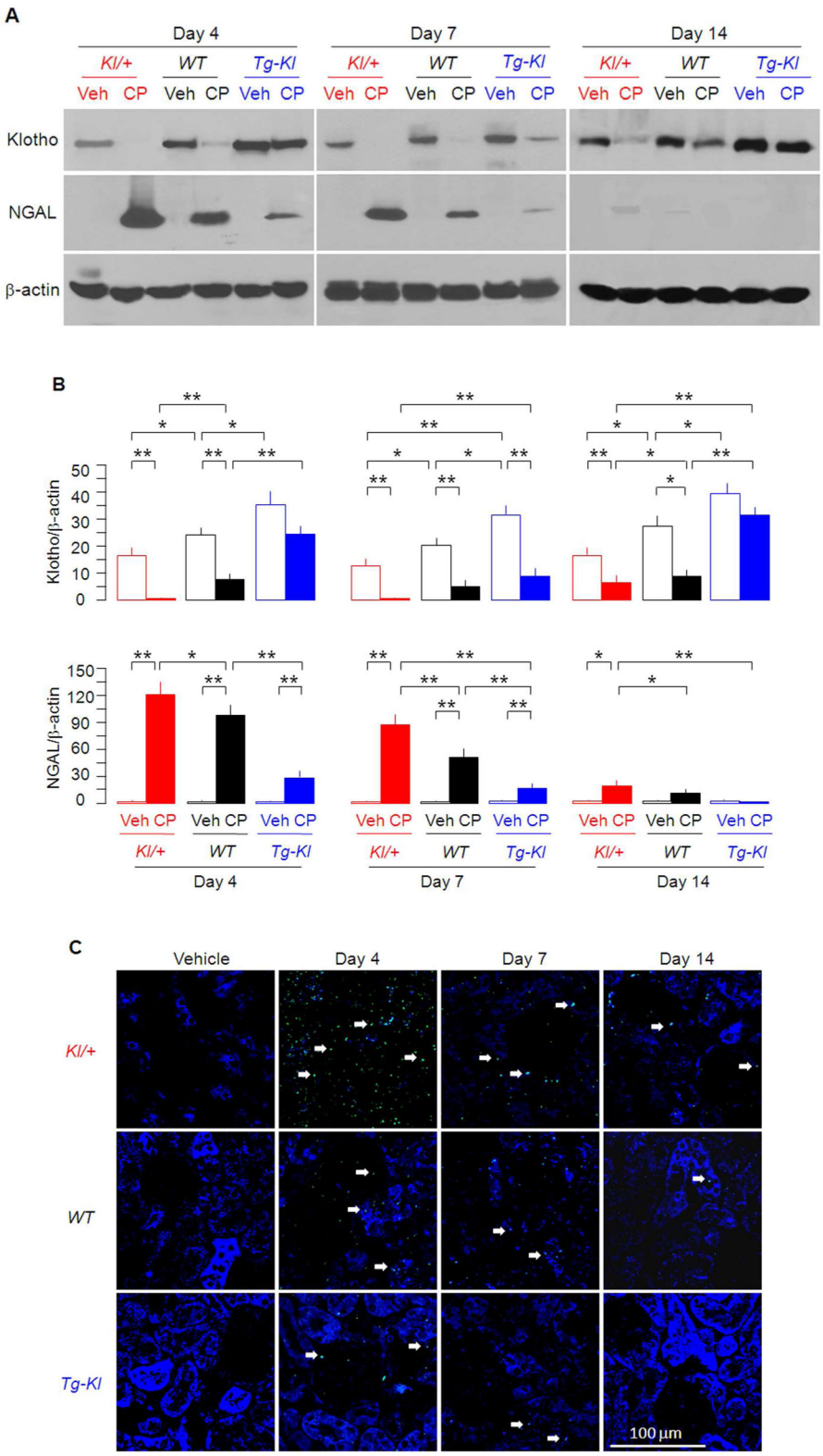

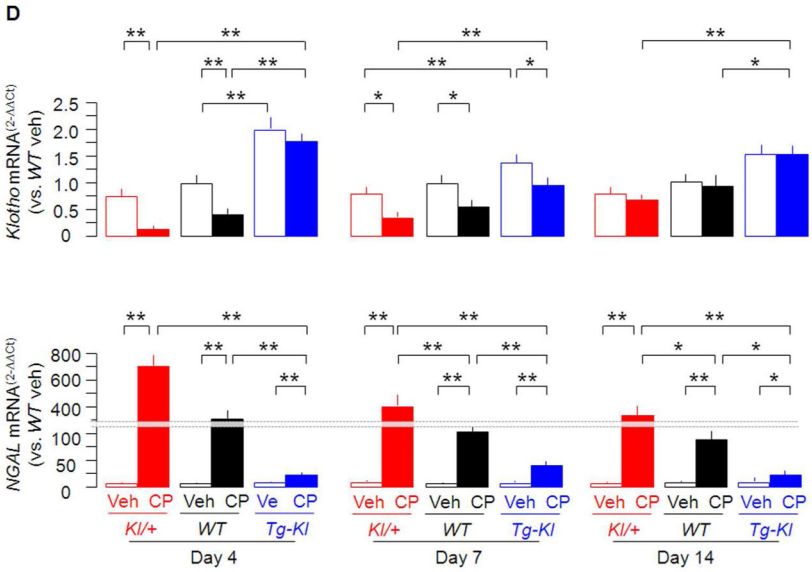

Figure 2. Cisplatin induces Klotho deficiency and increases NGAL expression

(**A**) Representative immunoblot for NGAL and Klotho in total kidney lysate in each group (total 4 mice per group) at day 4, 7 and 14 post cisplatin (CP) or vehicle injection. (**B**) Summarized densitometric analyses of all samples from vehicle or cisplatin injected mice. Data are expressed as means ± SD of 4 animals from each group. (**C**) Representative fluorescent immunohistochemistry for Klotho (blue) and NGAL (green) in paraffin kidney sections at day 4, 7 and 14 post injection (4 mice in each group). Arrows show NGAL signals. (**D**) Levels of *Klotho* and *NGAL* transcripts in the kidneys from vehicle or cisplatin injected mice at the 4th, 7th, and 14th day were analyzed by qPCR. The relative quantity of transcripts was calculated as $2^{-(\Delta\Delta Ct)}$ by normalization to cyclophilin vehicle-injected *WT* mice as reference in each time point. Data are expressed as means ± SD of 6 animals from each group. Statistical significance was assessed by one-way ANOVA followed by Student-Newman-Keuls test, and significant differences were accepted when *P<0.05; **P<0.01 between two groups.

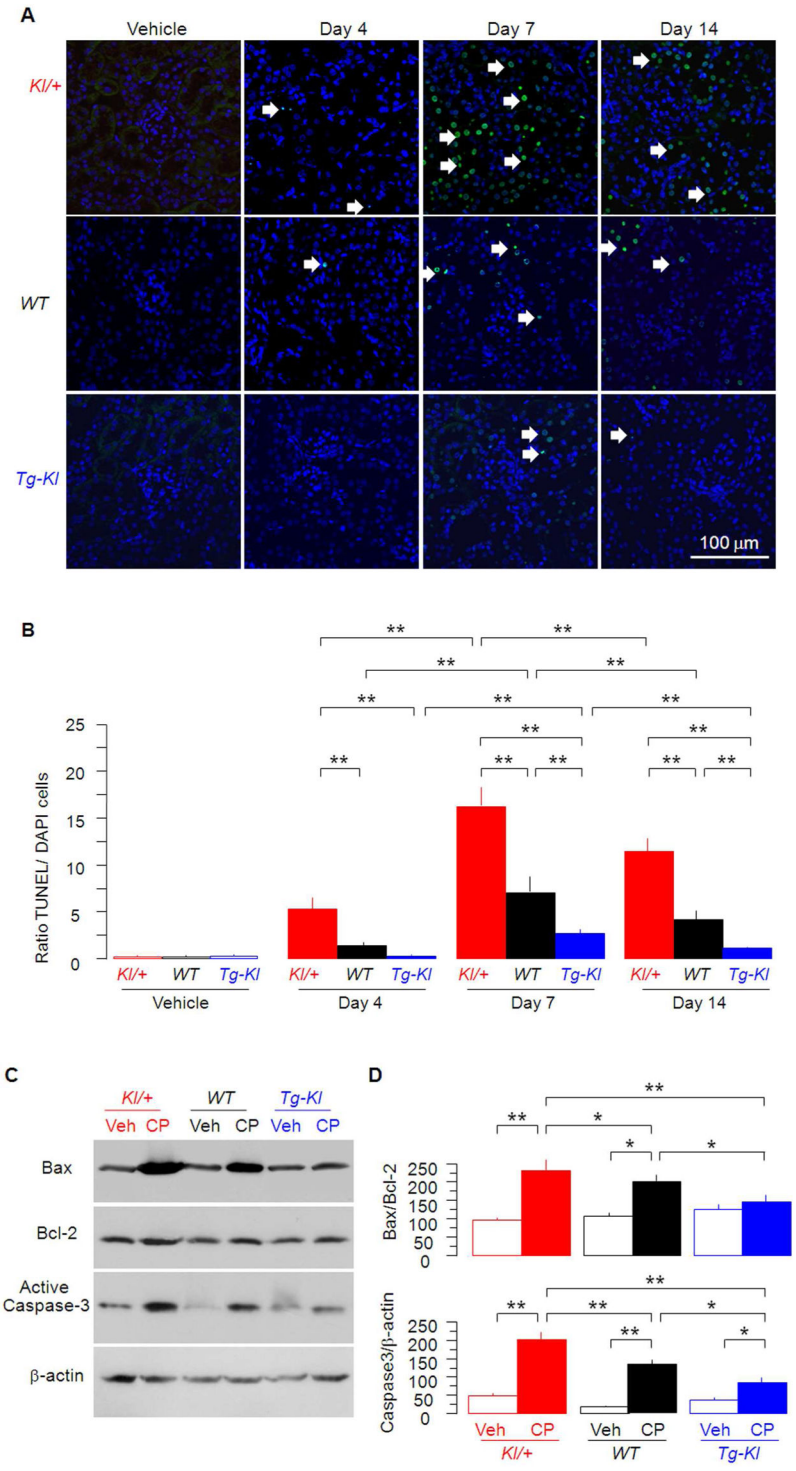

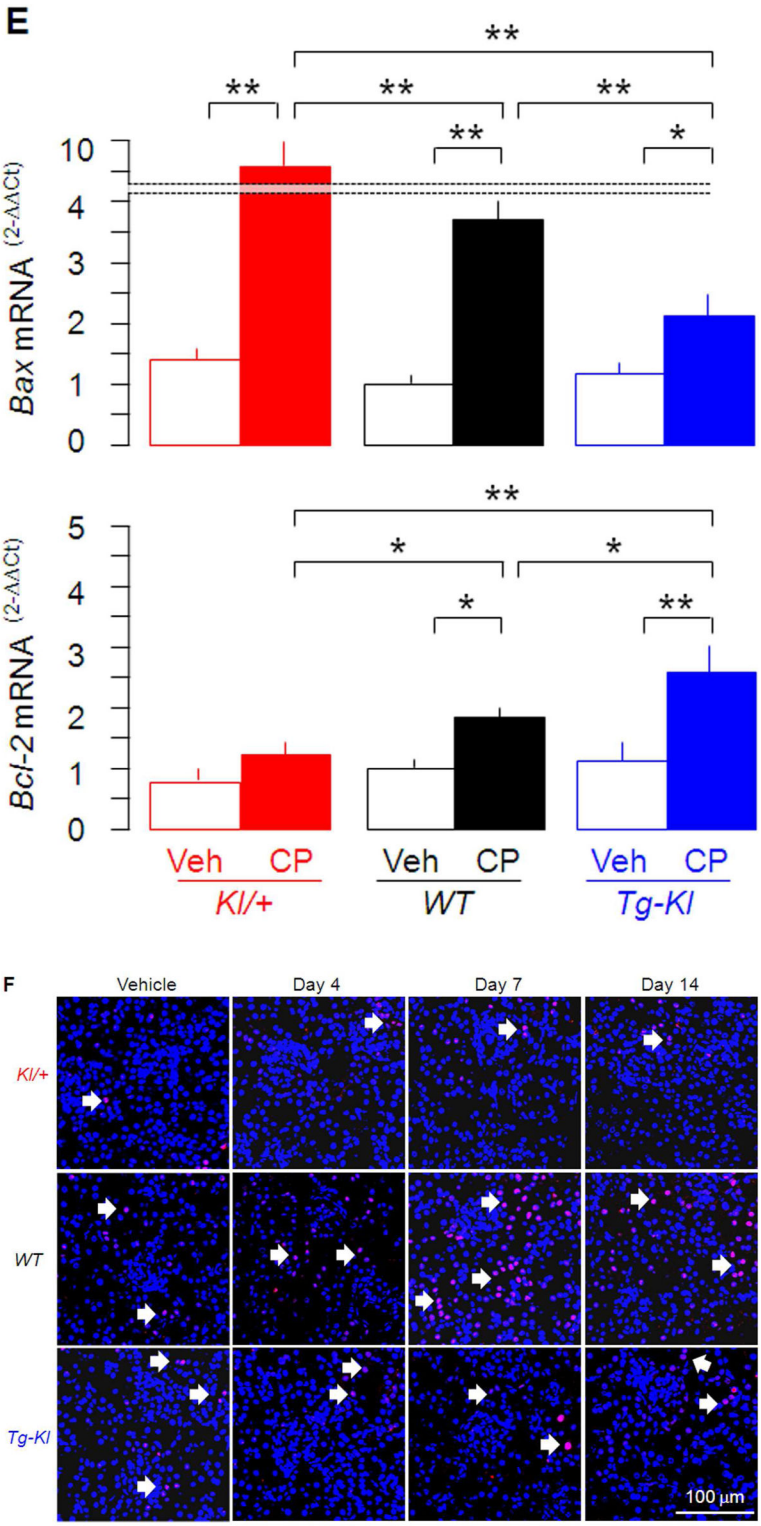

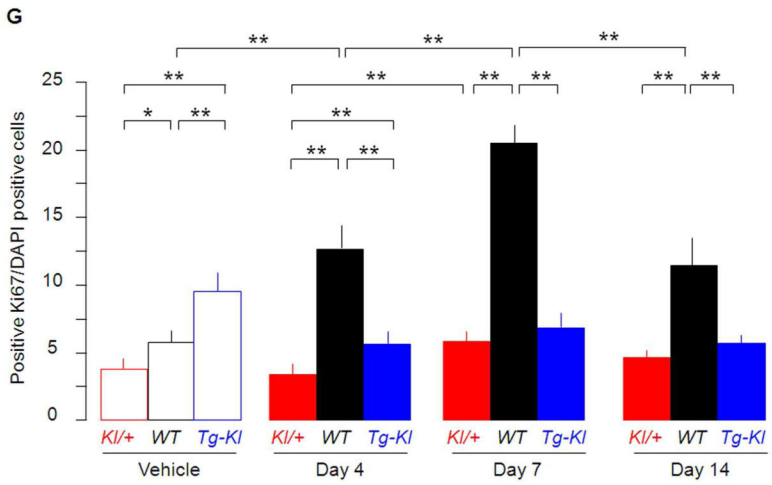

Figure 3. Klotho overexpression increases cell proliferation and suppresses cisplatin-induced apoptosis

(**A**) Representative fluorescent immunohistochemistry TUNEL (a cell apoptosis marker, green signal), and for DAPI (a marker of cell nuclei, blue signal) in paraffin-embedded kidney sections from each group (4 mice per group) at day 4, 7 and 14 post cisplatin (CP) or vehicle injection. Arrows show TUNEL-positive nuclei. (**B**) Summary of TUNEL-positive cells divided by total number of DAPI-positive cells from 10 microscopic fields at 40X magnification. Data are expressed as means ± SD of 4 animals from each group. (**C**) Representative immunoblot for Bax, Bcl-2, cleaved and active caspase-3, and β-actin in total kidney lysate from 4 mice kidneys in each group at day 7 post cisplatin injection. (**D**) Summarized densitometric analysis of all samples from vehicle or cisplatin injected mice. Data are expressed as means ± SD of 4 animals from each group. (**E**) Levels of *Bcl-2* and *Bax* mRNA in the kidneys from vehicle or cisplatin injected mice at the 7^{th} day were analyzed by qPCR with specific primers. The relative quantification of transcripts was calculated as $2^{-(\Delta\Delta Ct)}$ by normalization to cyclophilin and compared to vehicle injected *WT* mice in each study time point. Data are expressed as means ± SD of 6 animals from each group. (**F**) Representative fluorescent immunohistochemistry for Ki67 (cell proliferation marker, red) and for DAPI (marker of cell nuclei, blue) in paraffin-embedded kidney sections from each group (4 mice per group at days 0, 4, 7 and 14 post cisplatin or vehicle injection. Arrows show positive signal of Ki67. (**G**) Summary of positive Ki67 cells over total number of DAPI cells from 10 microscopic fields at 40X magnification. Data are expressed as means ± SD of 4 animals from each group. Statistical significance was assessed by one-way ANOVA followed by Student-Newman-Keuls test, and significant differences were accepted when *P<0.05; **P<0.01 between two groups.

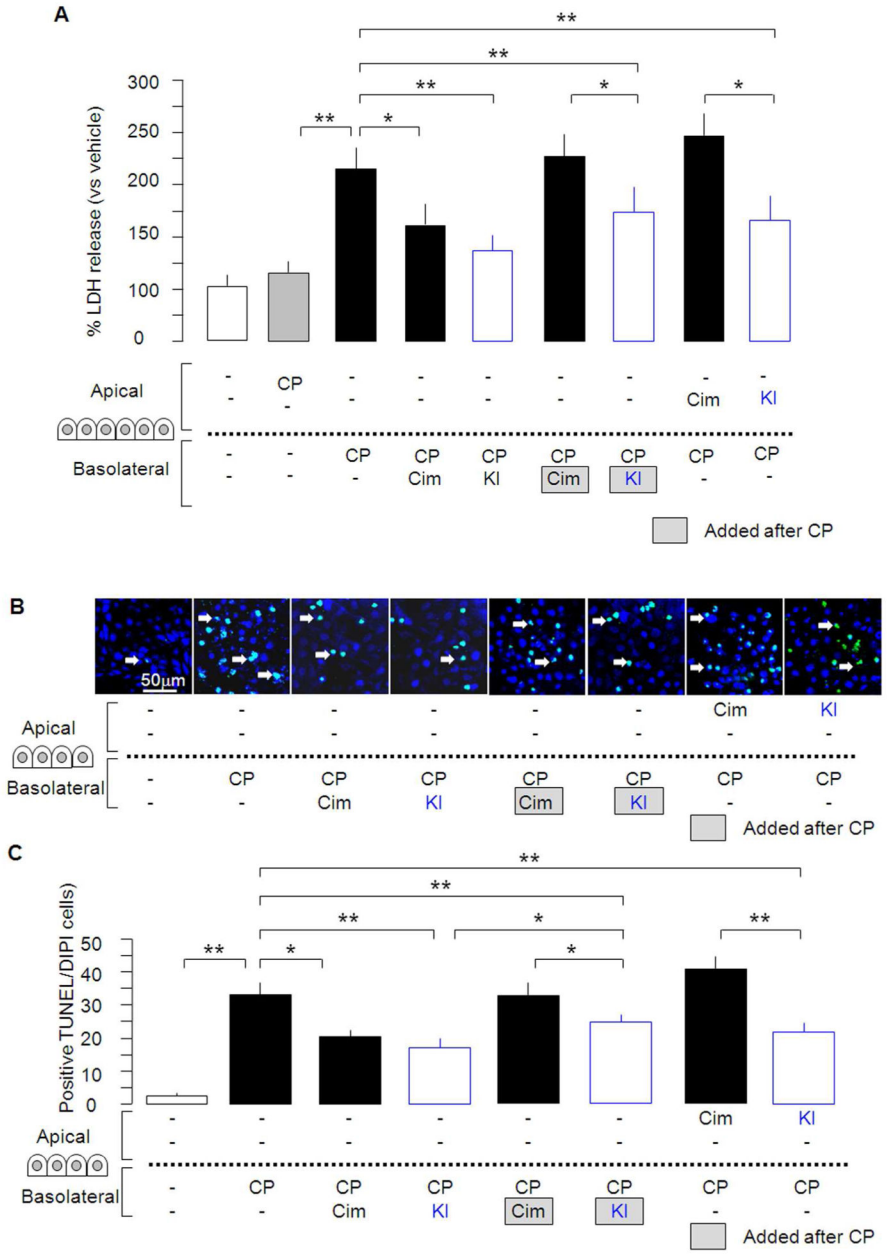

Figure 4. Klotho protects NRK cells from cisplatin cytotoxicity

NRK cells were plated on Transwell plate to allow separate access to apical and basal compartments. Cisplatin (CP), Klotho (Kl), or Cimetidine (Cim) were added to either apical or basolateral compartments simultaneously. Alternatively, Cisplatin was added basally for 20 minutes followed by wash-out and addition of cimetidine or Klotho to basal side. (**A**) Cell damage was measured by LDH release. (**B**) Representative fluorescent immunocytochemistry for TUNEL (apoptosis marker, green), and for DAPI (marker of cell nuclei, blue) in NRK cells from a total of 4 independent experiments. Arrows show positive TUNEL signal. (**C**) Summary of positive TUNEL cells divided by total number of DAPI cells from 5 microscopic fields at 40X magnification. In both (**A**) and (**C**), Data are

expressed as means ± SD of 4 independent experiments. Statistical significance was assessed by one-way ANOVA followed by Student-Newman-Keuls test, and significant differences were accepted when *P<0.05; **P<0.01 between two groups. Cim: cimetidine; Kl: Klotho; inhib.: inhibitor.

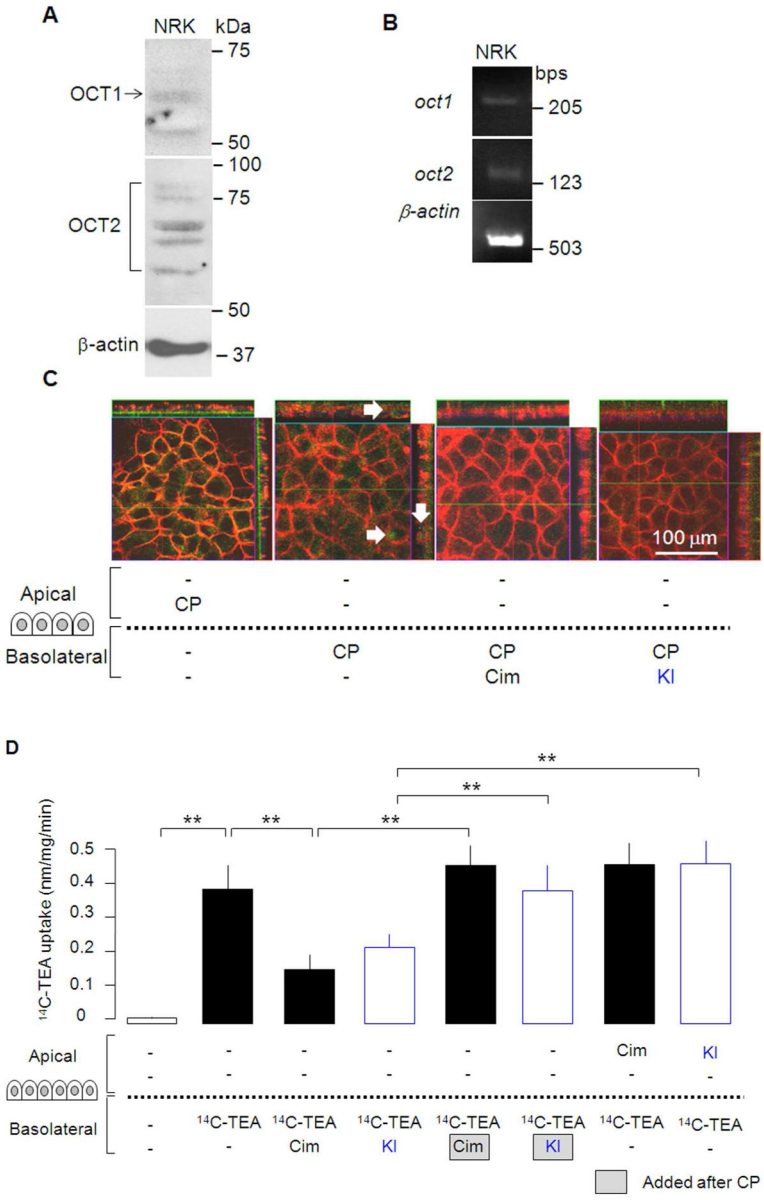

Figure 5. Klotho suppresses OCT-mediated cisplatin update by NRK cells

(**A**) Representative immunoblots for OCT1 and OCT2 protein expression in total cell lysate of NRK cells from 3 independent experiments. (**B**) Representative RT-PCR for *oct1*, *oct2*, and *β-actin* transcripts in NRK cells and kidneys of normal Spraque-Dalwey rat. Same findings were seen in 3 independent experiments. (**C**) Representative confocal images showing fluorescence-labeled cisplatin uptake by NRK cells. Cisplatin was labeled with Oregon Green 488 dye (Invitrogen) and added to apical or basolateral medium with Klotho or cimetidine or vehicle. Arrows show the presence of cisplatin in the cytoplasmic compartment of NRK cells. Same results were seen in 3 independent experiments. (**D**) ^{14}C-TEA was basally or apically incubated with cimetidine or Klotho simultaneously or ^{14}C-TEA was basally incubated for 20 minutes followed by wash-out and addition of cimetidine or Klotho to basal medium. Data are expressed as means ± SD of 4 independent

experiments. Statistical significance was assessed by one-way ANOVA followed by Student-Newman-Keuls test, and significant differences were accepted when *P<0.05; **P<0.01 between two groups. TEA: tetraethylammonium.

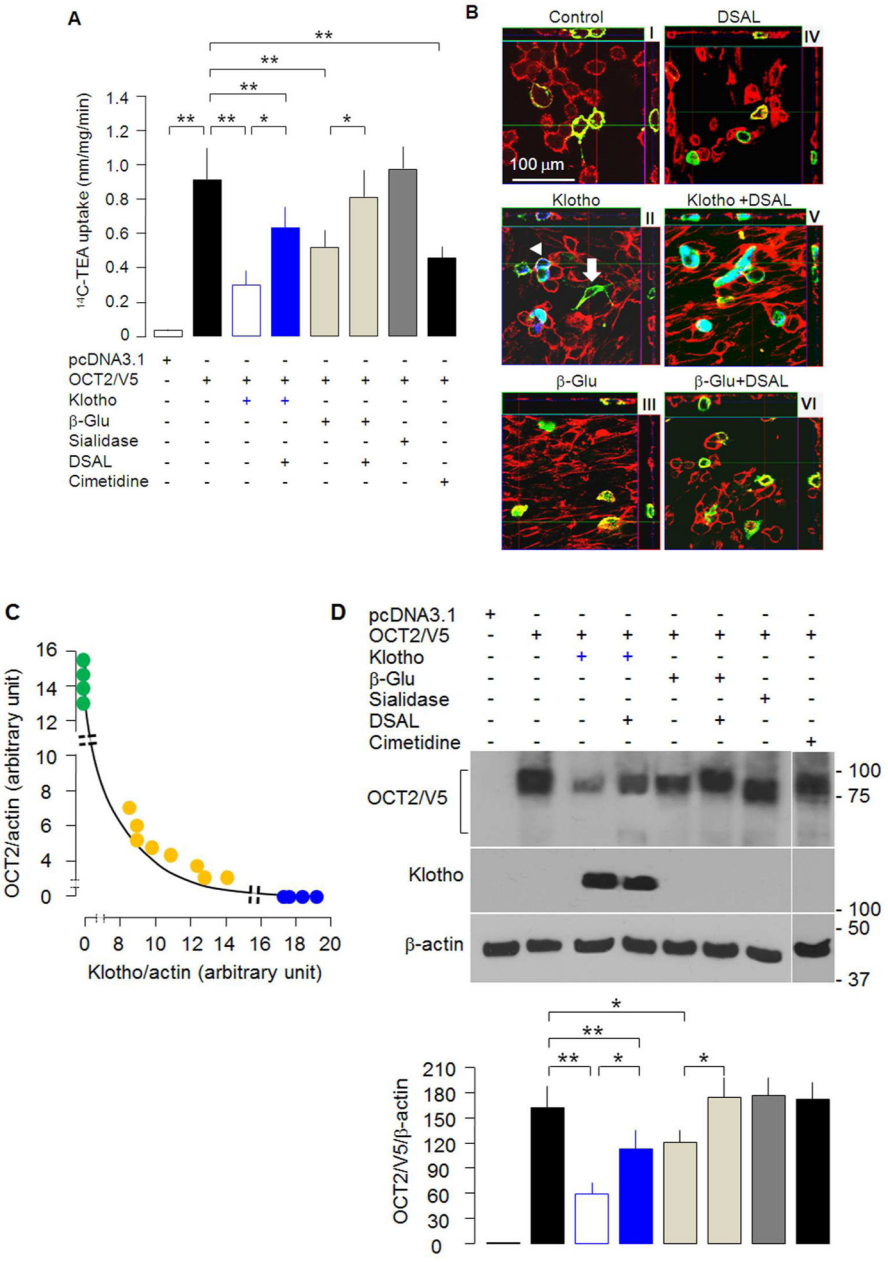

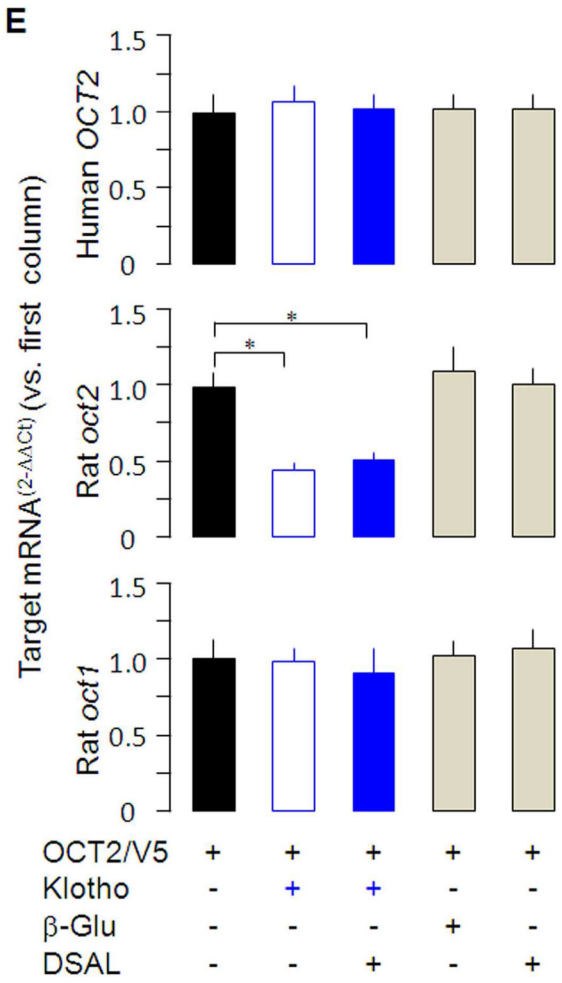

Figure 6. Mechanism of action of Klotho on OCT2 in CHO cells

CHO cells were transiently transfected with empty pcDNA3.1 vector, human OCT2-V5 plasmid, or human Klotho plasmid. Two days post-transfection, cells were subjected to ^{14}C-TEA uptake, immunocytochemistry, immunoblot, and RT-qPCR. β-glucuronidase (100μg/ml), sialidase (0.1 IU/ml), DSAL (10 μM), or cimetidine (0.1 mM) were added into culture medium 16 hours prior to assays. (**A**) ^{14}C-TEA uptake by CHO cells. Data are expressed as means ± SD of 4 independent experiments. (**B**) Representative image (X, Y and Z scanning) of fluorescent immunocytochemistry for V5 (OCT2, green), for Klotho (blue) and for phalloidin (marker of actin, red) in CHO cells from 4 independent experiments. CHO cell without Klotho expression had strong OCT2 expression (showed by arrow); whereas CHO cells expressing high Klotho had weak OCT2 expression (showed by arrow). (**C**) Summary of arbitrary units of OCT2 signal vs. Klotho signal in OCT2/V5 and/or Klotho transiently transfected CHO cells. Each point was an average of arbitrary units from 5 different randomized fields where each field has at least 4 positive transfected cells at 100X magnification. OCT2-positive cells (green symbols); Klotho-positive cells (blue symbols) and double positive cells (orange symbols). Y axis is arbitrary unit of OCT2 signal calculated by green density (OCT2) over red density (actin) using Image J program; X axis is arbitrary unit of Klotho signal which was calculated by green density (OCT2) over red

density (actin) using Image J program. Data are expressed as means ± SD of 4 independent experiments. (**D**) Representative immunoblots for OCT2/V5 by V5 antibody, Klotho by KM2076 antibody, and β-actin in total membrane protein extracted from CHO cells. Identical results were seen in 3 independent experiments. Bottom panel is a summary of densitometric analysis of bands of V5 and β-actin from all 3 independent experiments. (**E**) Levels of human *OCT2*, rat *oct1* and *oct2* mRNA in NRK cells transiently transfected with human OCT2/V5 plasmid and Klotho plasmid were quantitatively analyzed by qPCR with specific primers. The relative quantification of transcripts was calculated as $2^{-(\Delta\Delta Ct)}$ by normalization to cyclophilin and compared to OCT2/V5 transfected CHO cells. Data are expressed as means ± SD of 3 independent experiments. Statistical significance was assessed by one-way ANOVA followed by Student-Newman-Keuls test, and significant differences were accepted when *: $P<0.05$; or **: $P<0.01$ between two groups. β-glu: β-glucuronidase; DSAL: D-Saccharic acid 1,4-lactone.

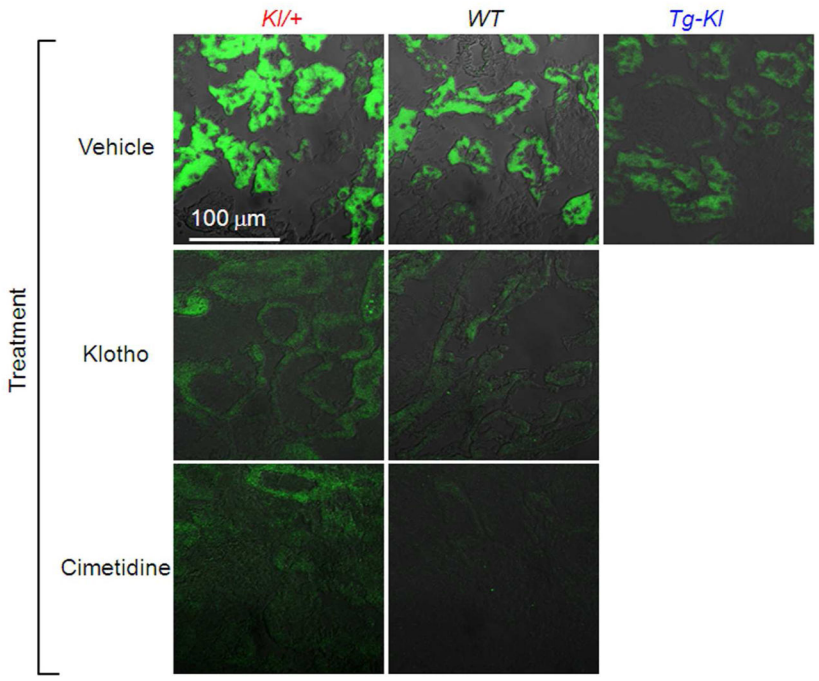

Figure 7. Klotho decreased cationic styryl dye (ASP^+, a substrate of OCT) uptake by kidney slices

Kidney slices from *Kl/+*, *WT*, and *Tg-Kl* (**C**) mice were co-incubated with ASP^+ with vehicle, Klotho, or cimetidine for 2 hour. Kidney sections were photographed for ASP^+ signal (green fluorescent) with laser confocal microscopy.

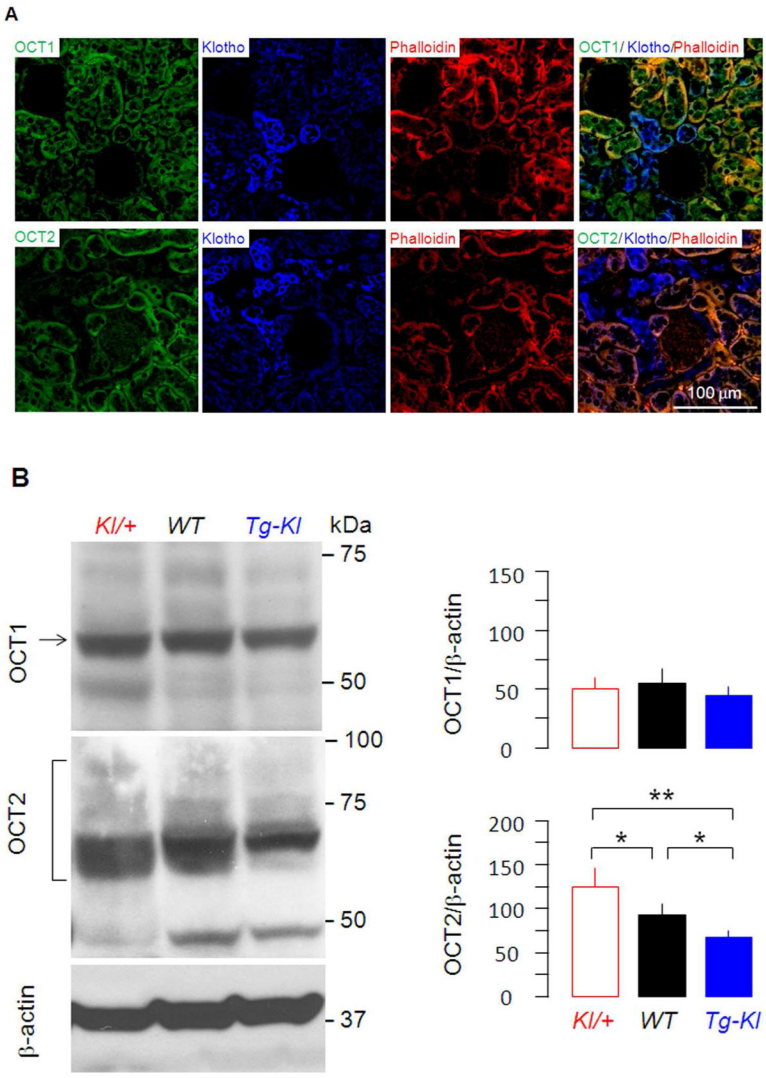

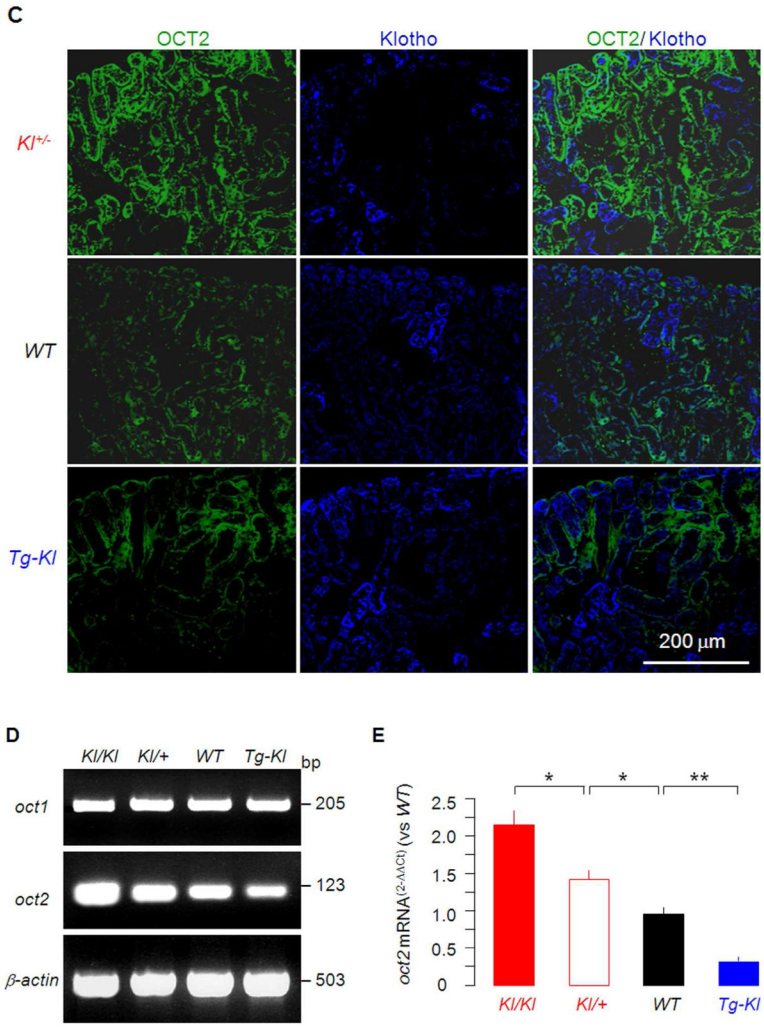

Figure 8. OCT1 and 2 are expressed in mouse kidney

(**A**) Representative fluorescent immunohistochemistry for OCT1 and OCT2 (green), Klotho (blue), and phalloidin (actin, red) in paraffin-embedded kidney sections from *WT* mice. (**B**) Representative immunoblots for OCT1, OCT2, and β-actin in total kidney lysate from 3 mice in each genotype. Right panel is a summarized densitometric analysis OCT1 and OCT2 protein over β-actin. Data are expressed as means ± SD of 3 animals from each genotype. (**C**) Representative fluorescent immunohistochemic stain for OCT2 (green) and Klotho (blue) in paraffin-embedded kidney sections from mice in each genotype. (**D**) Representative RT-PCR for *oct1*, *oct2*, and *β-actin* transcripts in the kidney from mice with each genotype. (**E**) The levels of *oct2* mRNA in mouse kidneys were quantitatively analyzed by RT-qPCR with specific primers. The relative quantification of transcripts was calculated as $2^{-(\Delta\Delta Ct)}$ by normalization to cyclophilin compared to *WT* mice. Data are expressed as means ± SD of 3 animals from each genotype. All experiments were repeated independently 3 times. Statistical significance was assessed by one-way ANOVA followed by Student-Newman-Keuls test, and significant differences were accepted when *P<0.05; **P<0.01 between two groups.

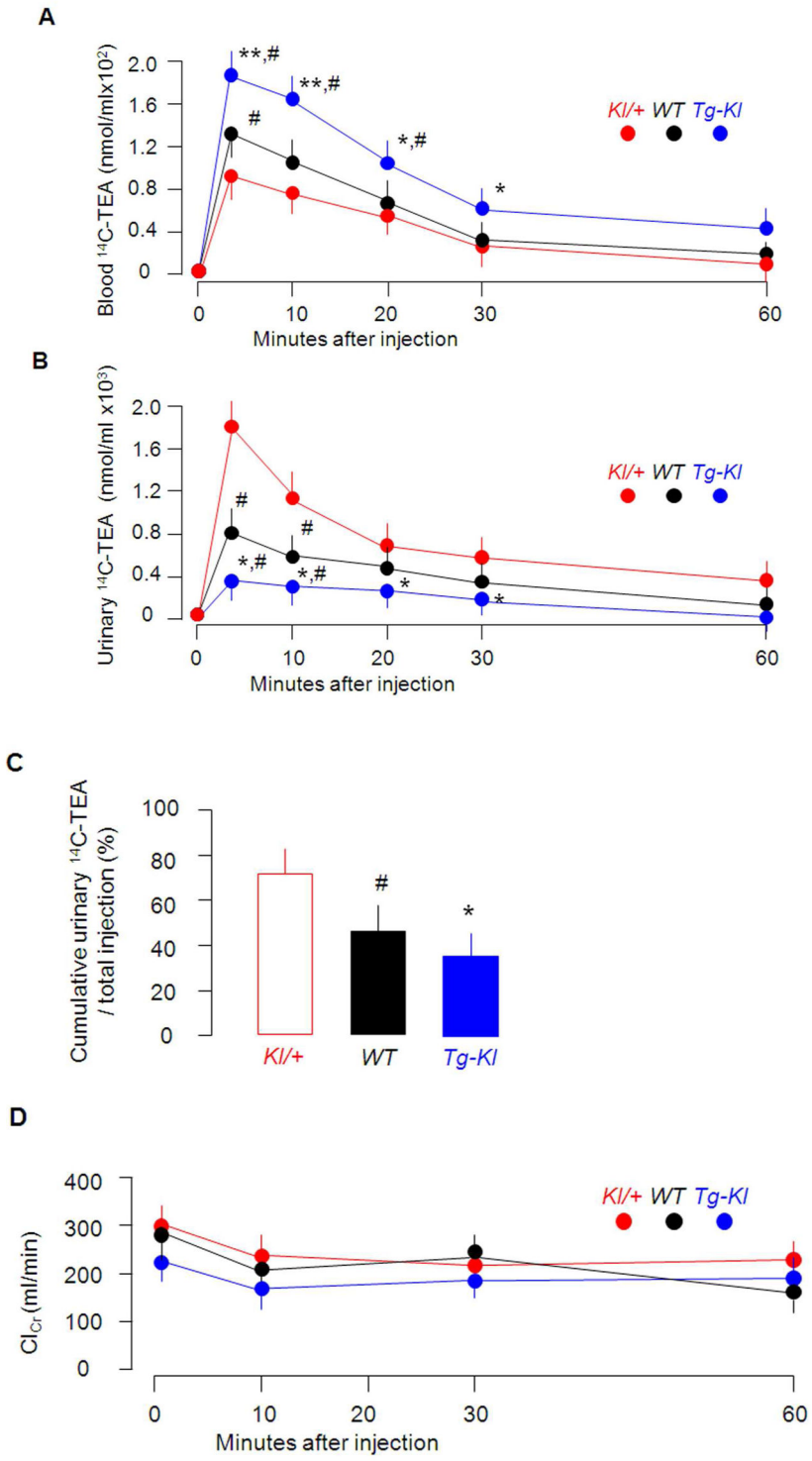

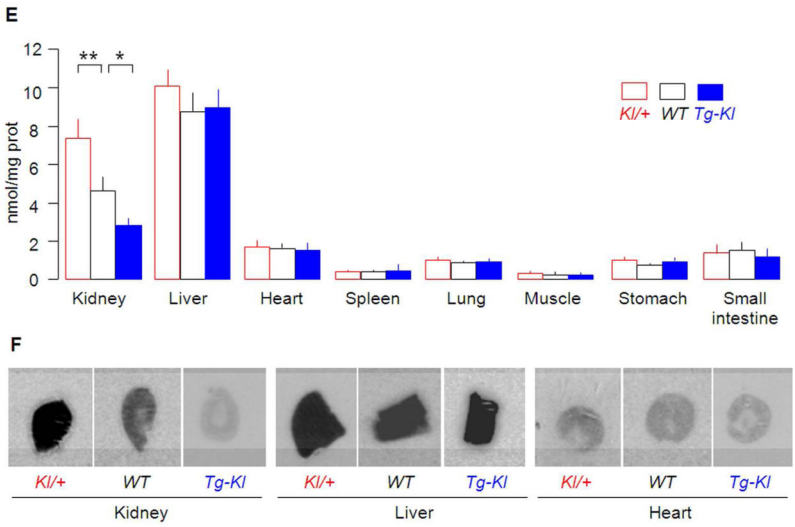

Figure 9. Klotho suppressed cisplatin excretion *in vivo*

Ten µl/gram BW of ^{14}C-TEA (0.1 µCi/µl, 3.5 mCi/mmol) was once injected intravenously into *Kl/+*, *WT* and *Tg-Kl* mice, blood and urine samples were collected at the indicated times. (**A**) Time course of blood concentration of ^{14}C-TEA. (**B**) Time course of urinary excretion of ^{14}C-TEA. (**C**) Cumulated urinary ^{14}C-TEA over 60 minutes. (**D**) Creatinine clearance. In **A–C**, data are expressed as means ± SD of 3 animals from each genotype and statistical analysis were run by one-way ANOVA followed by Student-Newman-Keuls test. Significant differences were accepted when *P<0.05; **P<0.01 compared to *Kl/+* mice; and when $^{\#}$:P<0.05; $^{\#\#}$:P<0.01 compared to *WT* mice. (**E**) Two hours after injection, eight organs were harvested and homogenized for measurement of ^{14}C-TEA uptake and total protein. Uptake of ^{14}C-TEA normalized to protein was calculated and significances between mice with three different genotypes were analyzed by one-way ANOVA followed by Student-Newman-Keuls test. Significant differences were accepted when *P<0.05; **P<0.01 between two groups. (**F**) Tissues and organs were sectioned at 10 µm thickness and subjected to autoradiography.

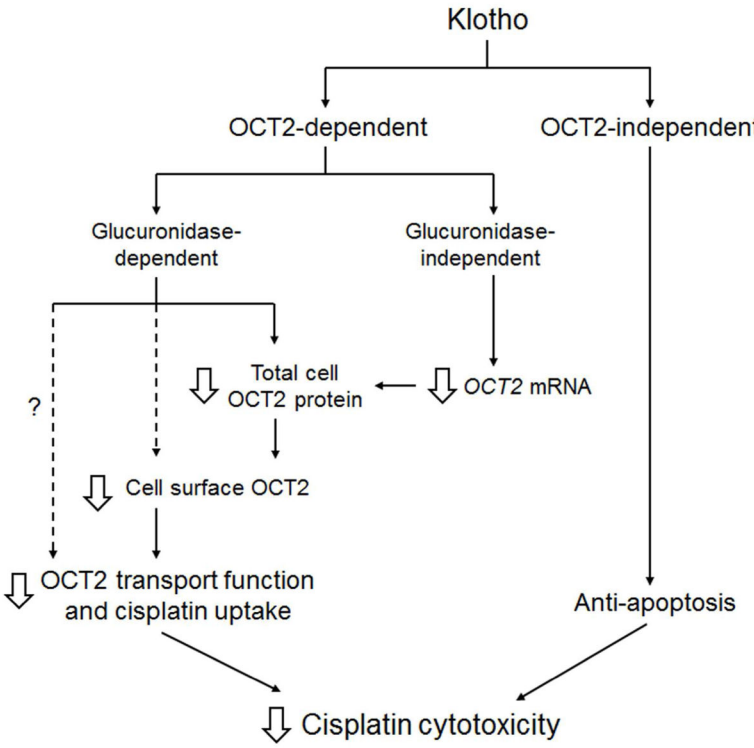

Figure 10. Summary of findings and proposed scheme for Klotho effect on cisplatin-induced cytotoxicity

Klotho OCT2-independent effect is related to anti-apoptosis (right panel). Klotho OCT2-depedent effects (let panel) can be glucuronidase-dependent or glucuronidase-independent. Glucuronidase-independent effect is associated with downregulation of *OCT2* mRNA. Glucuronidase-dependent effects are more complex. Klotho could decrease total cell OCT2 protein by functioning as a glucuronidase independent of *OCT2* mRNA. Klotho also reduces primarily glycosylated surface OCT2 protein in 2 hours effect, and both glycosylated and unglycosylated surface OCT2 in 2 days effect. Klotho can potentially directly decrease OCT2 activity without alteration of OCT2 protein (dash line). Collectively, Klotho suppresses OCT2 transport function and consequently reduces cisplatin uptake. On the other hand, Klotho functions as an anti-apoptotic agent and anti-oxidant independently of cisplatin uptake to protect cells against cisplatin-induced cytotoxicity.

Table 1

AUC_{0-60} of ^{14}C-TEA in blood and urine of mice

	Kl/+	WT	Tg-Kl
Blood ^{14}C-TEA (nmol/µl)	4.13±0.12 (3)	2.68±0.18 (3)**	2.22±0.12 (3)##
Urine excretion rate ^{14}C-TEA (pmol/mim)	3,38±0.18 (3)	2.08±0.08 (3)*	1.36±0.08 (3)**

Data are expressed as Mean ± SD (number of experiment). Statistical significance was assessed by one-way ANOVA followed by Student-Newman-Keuls test, and significant differences were accepted when

* P<0.05;

** P<0.01 vs *Kl/+* mice;

# P<0.05;

P<0.01 vs *WT* mice.